Majorana zero modes choose Euler numbers as revealed by full counting statistics

Dong E. Liu,[1] Alex Levchenko,[2,3] and Roman M. Lutchyn[1]
[1]*Station Q, Microsoft Research, Santa Barbara, California 93106-6105, USA*
[2]*Department of Physics, University of Wisconsin-Madison, Madison, Wisconsin 53706, USA*
[3]*Department of Physics and Astronomy, Michigan State University, East Lansing, Michigan 48824, USA*
(Received 13 March 2015; revised manuscript received 16 July 2015; published 18 November 2015)

We study transport properties of a quantum dot coupled to a Majorana zero mode and two normal leads. We investigate the full counting statistics of charge tunneling events and obtain complete information on current fluctuations through the dot. Using the Keldysh path-integral approach, we compute the cumulant generating function of the current. We first consider a spinless case and find that for the symmetric dot-lead couplings, the zero-frequency cumulants are independent of the microscopic parameters and exhibit a universal pattern described by Euler numbers. We then consider the spinful system and investigate the effect of both weak and strong Coulomb interactions. We show that cases with and without Majorana coupling exhibit qualitatively different full counting statistics of charge tunneling events despite the fact that differential linear conductance might have zero-bias features in both cases.

DOI: 10.1103/PhysRevB.92.205422 PACS number(s): 73.21.Hb, 71.10.Pm, 74.78.Fk, 72.70.+m

I. INTRODUCTION

Majorana zero-energy modes (MZMs) have recently attracted enormous theoretical and experimental attention [1–4] due to their exotic non-Abelian braiding statistics [5–7] and potential application to fault-tolerant topological quantum computation [8]. A large number of theoretical proposals has been put forward to realize MZMs in topological superconductors (TSCs) [9–17]; see also reviews [4,18,19] for more details. One of the most promising proposals involves a semiconductor nanowire with strong spin-orbit interaction coupled to a conventional s-wave superconductor [13,14]. An appropriate combination of the spin-orbit coupling, Zeeman splitting, and induced s-wave pairing allows one to realize an effectively spinless p-wave superconductivity at the interface which is characterized by the presence of MZMs bound to certain defects (i.e., vortices in two dimensions and domain walls in one dimension) [7,20]. The simplest way to detect MZMs is to measure local density of states at the defect and to probe the emergence of the zero-energy resonance across the topological phase transition. The first Majorana tunneling spectroscopy experiment, based on a semiconductor/superconductor heterostructure proposal [13,14], was performed in Delft [21]. Later on, the observation of the zero-bias peak in a finite magnetic field, consistent with the theoretical predictions [22], was reported by many other experimental groups [21,23–28]. The main challenge of these measurements is to exclude the other false-positive contributions to the zero-bias peak that are ubiquitous in condensed matter systems such as the Kondo effect [29,30], disorder in the topological region [31–35] and in the leads [36,37], as well as some other resonant Andreev scattering phenomena [19]. The feature distinguishing the Majorana origin of the zero-bias peak from the other mechanisms is the quantized zero-bias peak conductance of $2e^2/h$ which is a universal property of Majorana zero modes [38,39]. However, due to the large subgap conductance (so-called "soft gap" problem) observed in tunneling experiments [21,23–28], the largest observed height of the zero-bias peak was at most 30% of the predicted value. Therefore, additional experimental tests [37,40–55] are necessary in order to conclusively confirm the presence of MZMs in the semiconductor-superconductor heterostructures.

In this paper, we study current correlations in a mesoscopic device consisting of a quantum dot (QD) coupled to a MZM and two normal leads. The possibility of tuning the couplings between QD and other conductors as well as QD gate voltage allows one to study current correlations in a well-controlled environment. We show here that in the case of a symmetric left-right normal metal coupling (see Fig. 1 for a layout of the proposed device), current fluctuations are characterized by a universal pattern of the zero-frequency cumulants. We argue that the measurement of such cumulants allows one to exclude other false-positive signatures in tunneling transport and uniquely identify the presence of the putative Majorana modes.

The transport properties of a strongly interacting QD coupled to an MZM and a single normal lead (NL) have been studied using master equations, valid in the high-temperature regime, in Ref. [41]. The low-temperature behavior of the MZM-QD-NL system and the interplay between Kondo and Majorana couplings was considered in Ref. [43] finding that zero-bias tunneling conductance exhibits strong temperature dependence, which is distinct from that of a MZM-NL structure [38,39]. Later on, Cheng *et al.* [46] revisited the low-temperature behavior of the MZM-QD-NL system, and found that Majorana coupling significantly modifies the low-energy properties of the QD and drives the system to a new (different from Kondo) infrared fixed point. They also confirmed that the temperature dependence of the zero-bias conductance at the particle-hole symmetric point is similar to that of the MZM-NL structure [39]. The zero-bias conductance of a noninteracting QD with a side-coupled MZM (ungrounded TSC) through two normal leads was considered in Refs. [42,45], where it was predicted that the tunneling conductance is given by $e^2/2h$ for symmetric QD-lead couplings. Reference [44] considered a spinful QD in the Kondo regime for this two-lead structure, and studied the QD spectrum and zero-bias conductance by using the numerical renormalization group method, which shows that the zero-bias conductance is $3e^2/2h$ for small QD-MZM coupling. The shot noise of a different two-lead structure

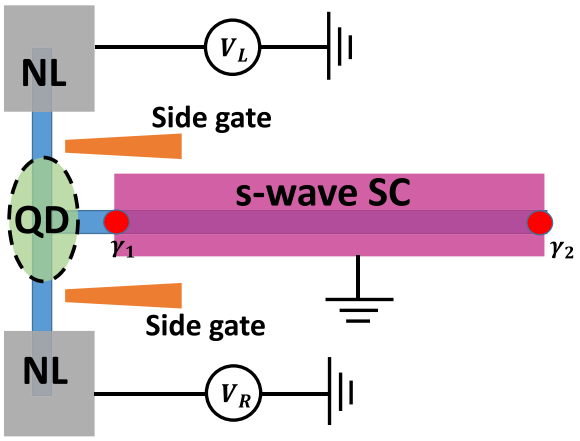

FIG. 1. (Color online) Proposed experimental setup to measure the distribution function of the transmitted charge, namely the full counting statistics. The QD is created near the center of the semiconductor nanowire T junction, two normal metal leads are attached to the upper and lower legs, and an s-wave superconductor is in proximity to the third lead. The latter realizes the topological superconductor hosting two MZMs γ_1 and γ_2.

(with a grounded TSC) has been studied in Ref. [56] for both noninteracting spinless QD and spinful Kondo QD predicting that the shot noise not only shows universal behaviors but also can be used for qualitatively distinguishing MZMs with other modes. There has been also an experimental interest in QD-superconductor devices. The interplay of the Kondo effect and superconductivity has been revisited in Refs. [28,29,57,58]. A natural realization for the proposed experimental setup (see Fig. 1) involves a T junction of the semiconductor nanowires which can be grown using the vapor-liquid-solid growth technique [59]. The QD can be created near the junction; two normal leads and the TSC are connected to each leg of the T junction. Another electron channel capacitively couples the junction, and can be used as a charge sensor to measure the charge distribution function. Thus, we believe that the setup we propose in the paper is within the experimental reach.

Although conductance and shot noise exhibit peculiar universal dependence due to the MZM coupling, it is insightful to obtain the full probability distribution function of the charge transferred through the QD, which can serve as the Majorana sensor. The theory of full counting statistics (FCS) [60–62] for charge transport in mesoscopic systems was established by analyzing nonequilibrium transport. A great effort has been made to investigate various aspects of FCS in a variety of systems theoretically [63–77] and experimentally [78–85]. Recently, the FCS calculation has also been considered for electron transport through multiterminal networks of MZMs [76], and for Quantum dot Majorana system in the high temperature regime [86]. In this paper, we study FCS of charge tunneling through a QD with a side-coupled TSC, or equivalently a QD coupled to a MZM, in the low temperature regime. The charge transport is measured between two normal leads. Here we assume that TSC is grounded so there is also Andreev current between (left) lead and the superconductor. Using the Keldysh path-integral approach [87], we compute the cumulant generating function. We first consider a noninteracting spinless QD, and find that for the symmetric dot-lead couplings, the zero-frequency cumulants exhibit a universal pattern described by Euler polynomial. This result is independent of the microscopic parameters such as the QD energy level and QD-MZM coupling. For a spinful QD with a small QD Zeeman splitting, we compute FCS in the regime of weak (perturbative regime) and strong (single-electron occupancy regime) Coulomb interactions. In the former case, we compute the interaction-induced correction to the cumulant generating function up to the leading order in U (i.e., U^2). In the latter case, we study the FCS due to the interplay between the Kondo and Majorana coupling.

The paper is organized as follows. In Sec. II, we review the formalism of the FCS calculation for the mesoscopic transport problem. In Sec. III, we introduce the QD-MZM model and compute the cumulant generating function for this model with noninteracting spinless QD. In Sec. IV, we consider the weak Coulomb interaction effect for a spinful QD, and compute the leading order interaction correction to the cumulant generating function by using a diagrammatic perturbation method. In Sec. V, we consider the strong Coulomb interaction effect for a spinful QD, and study how Kondo and Majorana couplings affect the FCS. Finally, the conclusions are shown in Sec. VI.

II. FULL COUNTING STATISTICS: GENERAL FORMALISM

In this section, we will review the formalism for calculating full counting statistics (FCS) of charge fluctuations in a mesoscopic system (we refer a reader to Ref. [88] for more details). Consider the distribution function $\mathcal{P}_q$ for q electrons to be transferred through a mesoscopic device within the measurement time $\mathcal{T}$. Here we assume that the measurement time is long enough ($\mathcal{T} \gg e/I$) so that the average number of electrons M transferred within $\mathcal{T}$ is large, i.e., $M \gg 1$. The distribution function $\mathcal{P}_q$ allows one to extract more information about the nature of the charge carriers as well as the statistics of the charge fluctuations. In particular, tails of the distribution contain information about the statistics of rare events. From the theoretical point of view, rather than $\mathcal{P}_q$, it is more convenient to compute the cumulant generating function (CGF) $\chi(\lambda)$, defined by a Fourier transform,

$$\chi(\lambda) = \sum_q e^{iq\lambda}\mathcal{P}_q. \tag{1}$$

Here the auxiliary variable λ represents a counting field. From the CGF, one can calculate the cumulants $\langle\langle \delta^n q\rangle\rangle$ (irreducible moments of $\mathcal{P}_q$),

$$\langle\langle \delta^n q\rangle\rangle = \frac{\partial^n}{\partial(i\lambda)^n}\ln\chi(\lambda)|_{\lambda=0}. \tag{2}$$

Thus, the average current and zero-frequency symmetrized current noise can be obtained by a simple differentiation:

$$I = \frac{1}{\mathcal{T}}\int_0^{\mathcal{T}} dt\langle\hat{I}(t)\rangle = \frac{-i}{\mathcal{T}}\frac{\partial\ln\chi}{\partial\lambda}\bigg|_{\lambda=0}, \tag{3}$$

$$S = \int_0^{\mathcal{T}} dt\langle\delta\hat{I}(t)\delta\hat{I}(0) + \delta\hat{I}(0)\delta\hat{I}(t)\rangle = \frac{-1}{\mathcal{T}}\frac{\partial^2\ln\chi}{\partial\lambda^2}\bigg|_{\lambda=0}. \tag{4}$$

The third cumulant and the fourth cumulant describe the asymmetry (or skewness) and the kurtosis (or sharpness) of

the distribution function, and can be also straightforwardly obtained using $\chi(\lambda)$.

In order to define the CGF in a proper way, Levitov and Lesovik introduced a "gedanken scheme," in which a spin-1/2 system magnetically couples to the electric current [60,61]. Based on their definition, the CGF in a Keldysh formalism is given by

$$\chi(\lambda) = \left\langle T_C \exp\left[-i\int_C dt\, H^{\lambda}(t)\right]\right\rangle, \tag{5}$$

with

$$H^{\lambda}(t) = H + \frac{\lambda(t)}{2}\hat{I}. \tag{6}$$

Here, the integration is preformed along the Keldysh contour C, T_C is time ordering; $\langle\cdots\rangle$ is the quantum-mechanical average [87]. The second term in Eq. (6) describes the interaction between the electron current and counting field, and $\lambda(t)$ has different sign on the two branches of the Keldysh contour, i.e., $\lambda(t) = \lambda^{(1)}$ for forward branch and $\lambda(t) = \lambda^{(2)}$ for backward branch with $\lambda^{(1)} = -\lambda^{(2)} = \lambda$.

III. FCS FOR A SPINLESS QD WITH SIDE-COUPLED MZM

A. Theoretical model

We now consider the setup shown in Fig. 1—a quantum dot (QD) is coupled to an end of a one-dimensional (1D) topological superconductor (TSC) hosting two Majorana zero modes (MZMs) γ_1 and γ_2 at the opposite ends. For pedagogical reasons, we first consider the spinless model for this setup (assuming that the Zeeman splitting is very large), and relegate the discussion of the spinful case to the next sections. In the former case, the model is essentially noninteracting, and one can calculate FCS exactly. The QD is coupled to two normal spinless leads which can be used for transport measurements. Given that each lead couple to the QD at a single point, one can perform an unfolding transformation and reduce the problem to the one corresponding to a quantum impurity coupled to one-dimensional free fermions. Thus, the corresponding Hamiltonian reads

$$H = H_{\text{Lead}} + H_{\text{QD-MZM}} + H_{\text{T}}, \tag{7}$$

where the Hamiltonians for the leads, QD-MZM system, and the lead-QD couplings are, respectively, given by

$$H_{\text{Lead}} = -i v_F \sum_{\alpha=L,R}\int dx\, \psi_{\alpha}^{\dagger}(x)\partial_x\psi_{\alpha}(x), \tag{8}$$

$$H_{\text{QD-MZM}} = \epsilon_d d^{\dagger}d + i\kappa(d+d^{\dagger})\gamma_1 + i\delta\gamma_1\gamma_2, \tag{9}$$

$$H_{\text{T}} = \sum_{\alpha=L,R}(t_{\alpha}\psi_{\alpha}^{\dagger}(0)d + t_{\alpha}^{*}d^{\dagger}\psi_{\alpha}(0)). \tag{10}$$

Here $\psi_{\alpha}^{\dagger}$ ($d^{\dagger}$) is the creation operator for an electron in the α lead (QD), ϵ_d is the energy level in the QD, and $t_{\alpha k}$ (κ) is the tunnel coupling between the leads (MZM) and the QD. The effective Hamiltonian for the TSC is given in terms of the low-energy degrees of freedom (MZMs) assuming that the induced superconducting gap Δ is the largest energy scale in the problem. For a finite-length L TSC, the coupling δ between two MFs is exponentially small $\delta \sim \Delta\exp(-L/\xi)$ with the coherence length being $\xi = v_F/\Delta$.

We now derive the CGF for our QD-MZM model assuming the symmetric source-drain bias ($\mu_L = eV/2$ and $\mu_R = -eV/2$). The Hamiltonian including the counting field can be written as

$$H^{\lambda}(t) = H + \sum_{\alpha=L,R}\frac{\lambda_{\alpha}(t)}{2}\hat{I}_{\alpha}, \tag{11}$$

where the current operator for the α junction is $\hat{I}_{\alpha} = ie[H,N_{\alpha}]$ with the electron number operator N_{α} for the α lead. One can apply a gauge transformation to remove the last term in the $H^{\lambda}(t)$, and obtain

$$H^{\lambda} = H_{\text{Lead}} + H_{\text{QD-MZM}} + H_{\text{T}}^{\lambda}, \tag{12}$$

$$H_{\text{T}}^{\lambda} = \sum_{\alpha=L,R}(t_{\alpha}e^{-i\lambda_{\alpha}(t)/2}\psi_{\alpha}^{\dagger}(0)d + \text{H.c.}). \tag{13}$$

We note that for $\kappa = 0$, the gauge symmetry of the Hamiltonian allows one to gauge away one of the counting fields so it is enough to keep the counting field in one of the junctions. In the general case (i.e., $\kappa \neq 0$), however, we need to keep both counting fields λ_{α}.

We can now compute the path integral for the effective action defined by the Hamiltonian (12). Given that the presence of the superconductor (i.e., MZM coupling) breaks particle number conservation, the QD Green function contains anomalous contributions, e.g., $\langle T_C d(t)d(t')\rangle \neq 0$. Therefore, we introduce Nambu spinors: $\vec{\Psi}_{\alpha}^{\dagger} = (\psi_{\alpha}^{\dagger},\psi_{\alpha})/\sqrt{2}$ and $\vec{\Psi}_{d}^{\dagger} = (d^{\dagger},d)/\sqrt{2}$, where $\alpha = L,R$ is the lead index. The effective Keldysh action now reads

$$S = S_{\text{Leads}} + S_{\text{QD-MZM}} + S_{\text{T}}, \tag{14}$$

where

$$S_{\text{Leads}} = \sum_{\alpha}\int_C\int_C dt dt'\,\vec{\Psi}_{\alpha}^{\dagger}(t)\check{Q}_{0,\alpha}^{-1}(t,t')\,\vec{\Psi}_{\alpha}(t'),$$

$$S_{\text{QD-MZM}} = \int_C\int_C dt dt'\,\vec{\Psi}_{d}^{\dagger}(t)\,\check{Q}_{0,dd}^{-1}(t,t')\,\vec{\Psi}_{d}(t'), \tag{15}$$

$$S_{\text{T}} = -\sum_{\alpha}\int_C dt\left(t_{\alpha}e^{-i\frac{\lambda_{\alpha}(t)}{2}}\psi_{\alpha}^{\dagger}d + \text{c.c.}\right) \tag{16}$$

$$= -\sum_{\alpha}\int_C dt(\vec{\Psi}_{\alpha}^{\dagger}(t)M_{T,\alpha}\vec{\Psi}_{d}(t) + \text{H.c.}) \tag{17}$$

are the actions for leads, QD, and lead-QD coupling, and

$$M_{T,\alpha} = \begin{pmatrix} t_{\alpha}e^{-i\frac{\lambda_{\alpha}(t)}{2}} & 0 \\ 0 & -t_{\alpha}^{*}e^{i\frac{\lambda_{\alpha}(t)}{2}}\end{pmatrix}. \tag{18}$$

Here we have already integrated out the bulk degrees of freedom in the leads and kept only the field $\vec{\Psi}_{\alpha}^{\dagger}(t)$ at the $x = 0$, i.e., at the QD. The free lead Green's function $\check{Q}_{0,\alpha}$ at $x = 0$ in the Nambu space $\mathbb{N}$ can be written as

$$\check{Q}_{0,\alpha}(\omega) = \begin{pmatrix} g_{\alpha}^{0}(\omega) & 0 \\ 0 & \widetilde{g}_{\alpha}^{0}(\omega)\end{pmatrix}, \tag{19}$$

where $\widetilde{g}_{\alpha}^{0}(t-t')$ is the P-H conjugation of $g_{\alpha}^{0}(t-t')$. We perform Larkin-Ovchinnikov (L-O) rotation, and the Green

function in Keldysh space becomes

$$g^0_\alpha(\omega) = -i\pi\rho_F \begin{pmatrix} 1 & 2(1-2n_\alpha) \\ 0 & -1 \end{pmatrix}, \tag{20}$$

$$\widetilde{g}^0_\alpha(\omega) = -i\pi\rho_F \begin{pmatrix} 1 & 2(1-2\widetilde{n}_\alpha) \\ 0 & -1 \end{pmatrix}. \tag{21}$$

One notices that $g^{0,R}_\alpha(\omega) = -\widetilde{g}^{0,A}_\alpha(-\omega)$ and $g^{0,K}_\alpha(\omega) = -\widetilde{g}^{0,K}_\alpha(-\omega)$. Here, n_α is the Fermi distribution function of the α lead with chemical potential μ_α, and $\widetilde{n}_\alpha$ corresponds to the Fermi distribution function with $-\mu_\alpha$. Assuming the symmetric source-drain bias $\mu_L = eV/2$ and $\mu_R = -eV/2$, one can relate the Fermi function for particles and holes $\widetilde{n}_L = n_R$ and $\widetilde{n}_R = n_L$. The free QD Green function (with MZM coupling) can be written as

$$\check{Q}_{0,dd}(\omega) = \begin{pmatrix} G^R_{0,d\bar{d}} & G^K_{0,d\bar{d}} & F^R_{0,dd} & F^K_{0,dd} \\ 0 & G^A_{0,d\bar{d}} & 0 & F^A_{0,dd} \\ F^R_{0,\bar{d}\bar{d}} & F^K_{0,\bar{d}\bar{d}} & G^R_{0,\bar{d}d} & G^K_{0,\bar{d}d} \\ 0 & F^A_{0,\bar{d}\bar{d}} & 0 & G^A_{0,\bar{d}d} \end{pmatrix}, \tag{22}$$

where the retarded components read [41,56]

$$G^R_{0,d\bar{d}}(\omega) = \frac{\omega + i\eta_S + \epsilon_d - \Sigma_{\rm M}(\omega)}{(\omega + i\eta_S - 2\Sigma_{\rm M}(\omega))(\omega + i\eta_S) - \epsilon_d^2}, \tag{23}$$

$$G^R_{0,\bar{d}d}(\omega) = \frac{\omega + i\eta_S - \epsilon_d - \Sigma_{\rm M}(\omega)}{(\omega + i\eta_S - 2\Sigma_{\rm M}(\omega))(\omega + i\eta_S) - \epsilon_d^2}, \tag{24}$$

$$F^R_{0,dd}(\omega) = F^R_{0,\bar{d}\bar{d}}(\omega) = \frac{-\Sigma_{\rm M}(\omega)}{(\omega + i\eta_S - 2\Sigma_{\rm M}(\omega))(\omega + i\eta_S) - \epsilon_d^2}. \tag{25}$$

Here the self-energy due to MZM coupling is $\Sigma_{\rm M}(\omega) = \kappa^2\omega/(\omega^2 - \delta^2)$, and the infinitesimal $\eta_S \to 0$. The Keldysh components are proportional to η_S, and, thus, can be set to zero. After L-O rotation, the action for the tunneling part becomes

$$S_{\rm T} = -\sum_\alpha \int_{-\infty}^{\infty} dt \left[\vec{\Psi}^\dagger_\alpha \left(\sum_{i=cl,q} M^i_{T,\alpha} \otimes \gamma^i \right) \vec{\Psi}_d + \vec{\Psi}^\dagger_d \left(\sum_{i=cl,q} M^i_{T,\alpha} \otimes \gamma^i \right)^\dagger \vec{\Psi}_\alpha \right], \tag{26}$$

where

$$M^{cl}_{T,\alpha} = \begin{pmatrix} \frac{e^{-i\lambda^{(1)}_\alpha} + e^{-i\lambda^{(2)}_\alpha}}{2} & 0 \\ 0 & -\frac{e^{i\lambda^{(1)}_\alpha} + e^{i\lambda^{(2)}_\alpha}}{2} \end{pmatrix}, \tag{27}$$

$$M^{q}_{T,\alpha} = \begin{pmatrix} \frac{e^{-i\lambda^{(1)}_\alpha} - e^{-i\lambda^{(2)}_\alpha}}{2} & 0 \\ 0 & -\frac{e^{i\lambda^{(1)}_\alpha} - e^{i\lambda^{(2)}_\alpha}}{2} \end{pmatrix} \tag{28}$$

are written in the Nambu space whereas $\gamma^{cl} = \mathbb{I}$ and $\gamma^q = \sigma_1$ represent the Keldysh space. Note the relationship $\lambda^{(1)}_\alpha = -\lambda^{(2)}_\alpha = \lambda_\alpha$ which allows one to simplify the expressions. After some manipulations, the cumulant generating function can be written as

$$\chi(\lambda) = \int D[d^\dagger, d] D[\psi^\dagger_\alpha, \psi_\alpha] e^{i(S_{\rm Leads} + S_{\rm QD\text{-}MZM} + S_{\rm T})}. \tag{29}$$

Next, we perform Gaussian integration to find

$$\ln\chi(\lambda) = \frac{\mathcal{T}}{2} \int_{-\infty}^{\infty} \frac{d\omega}{2\pi} \ln\left[\frac{\det[\check{\mathbb{I}}_{4\times4} - \check{Q}_{0,dd}\check{Q}_{M\lambda}]}{\det[\check{\mathbb{I}}_{4\times4} - \check{Q}_{0,dd}\check{Q}_{M0}]} \right], \tag{30}$$

where

$$\check{Q}_{M\lambda} = \sum_\alpha \left(\sum_i M^i_{T,\alpha} \otimes \gamma^i \right)^\dagger \check{Q}_{0,\alpha} \left(\sum_i M^i_{T,\alpha} \otimes \gamma^i \right). \tag{31}$$

Equation (30) is a general expression for the CGF. In the next sections, we will explicitly evaluate $\chi(\lambda)$ for different limiting cases.

B. Results and discussions

1. QD coupled to two normal leads

It is instructive to review first a simple case of a noninteracting QD coupled to two normal leads. Taking the limit $\kappa = 0$ in Eq. (22) and substituting it into Eq. (30), one obtains

$$\ln\chi = \frac{\mathcal{T}}{2} \int_{-\infty}^{\infty} \frac{d\omega}{2\pi} \ln[(1+\Upsilon_+)(1+\Upsilon_-)], \tag{32}$$

with the functions $\Upsilon_\pm$ being defined as

$$\Upsilon_\pm = \frac{4\Gamma_L\Gamma_R}{(\omega \pm \epsilon_d)^2 + (\Gamma_L + \Gamma_R)^2} \times [n_L(1-n_R)(e^{i(\lambda_L - \lambda_R)} - 1) + R \leftrightarrow L]. \tag{33}$$

The term in the second bracket of the logarithm function in Eq. (32) is the particle-hole conjugation of the term in the first bracket. Since we consider a symmetric source-drain bias ($eV_L = -eV_R = eV/2$), the transformation $\omega \to -\omega$ (e.g., for the terms in the second bracket) will result in the following changes: $n_L \to 1 - n_R$ and $n_R \to 1 - n_L$. Thus, one can see that Eq. (32) is consistent with the results of Ref. [68]. Indeed, at zero temperature and to the linear order in applied bias eV, one obtains the well-known result for the shot noise in a QD:

$$\frac{S_{\rm LL}}{eV} = \frac{e^2}{h}(-i)^2 \frac{\partial^2 \ln\chi(\lambda_L, \lambda_R = 0)}{\partial\lambda_L^2}\bigg|_{\lambda_L=0} = \frac{2e^2}{h} \frac{4\Gamma_L\Gamma_R\left[(\Gamma_L - \Gamma_R)^2 + \epsilon_d^2\right]}{\left[\epsilon_d^2 + (\Gamma_L + \Gamma_R)^2\right]^2}. \tag{34}$$

One can notice that the shot noise (as well as other cumulants) generically depend on the microscopic parameters for the QD such as, for example, ϵ_d. Furthermore, in the resonant case corresponding to $\epsilon_d = 0$ and $\Gamma_L = \Gamma_R$, the first eight cumulants are given by

$$\{C_1(0), \ldots C_8(0)\} = \{1,0,0,0,0,0,0,0\}, \tag{35}$$

with $C_n(0)$ being defined as

$$C_n(0) = \frac{\langle\langle \delta^n q \rangle\rangle}{M}. \tag{36}$$

Notice that at the symmetric point $\Gamma_R = \Gamma_L$, all higher order ($n > 1$) cumulants become zero as $\epsilon_d \to 0$. This dependence on ϵ_d is a generic feature because density of states in QD strongly depends on the gate voltage controlling ϵ_d. As we show below, this is not the case when QD is coupled to a TSC.

2. QD coupled to two normal leads and a TSC

Let us now consider a QD coupled to a TSC through MZM coupling, i.e., $\kappa \neq 0$. Substituting Eqs. (19), (22), (27), and (28) into Eq. (30), we find the following expression for the cumulant generating function:

$$\ln \chi(\lambda) = \frac{\mathcal{T}}{2}\int_{-\infty}^{\infty}\frac{d\omega}{2\pi}\ln\Big[1-\frac{\mathbb{C}_1}{\mathbb{K}(\lambda=0)}n_L(1-n_L)-\frac{\mathbb{C}_2}{\mathbb{K}(\lambda=0)}n_R(1-n_R)+\frac{\mathbb{B}_1}{\mathbb{K}(\lambda=0)}n_L(1-n_R) + \frac{\mathbb{B}_2}{\mathbb{K}(\lambda=0)}n_R(1-n_L)+\frac{\mathbb{F}}{\mathbb{K}(\lambda=0)}n_Ln_R(1-n_L)(1-n_R)+\frac{\mathbb{J}}{\mathbb{K}(\lambda=0)}n_Ln_R(n_L-n_R)\Big]. \tag{37}$$

The coefficients ($\mathbb{C}_1$, $\mathbb{C}_2$, $\mathbb{B}_1$, $\mathbb{B}_2$, $\mathbb{F}$, $\mathbb{J}$, $\mathbb{K}$) in Eq. (37) are defined in the Appendix-A. Above expression can be simplified in the zero-temperature limit where the terms proportional to $n_L(1-n_L)$, $n_R(1-n_R)$, $n_Ln_R(1-n_L)(1-n_R)$, and $n_Ln_R(n_L-n_R)$ vanish, and and the corresponding expression for $\ln\chi(\lambda)$ becomes

$$\ln\chi(\lambda)|_{T\to 0} = \frac{\mathcal{T}}{2}\int_{-\infty}^{\infty}\frac{d\omega}{2\pi}\ln[1+\mathbb{N}_1n_L(1-n_R)+\mathbb{N}_2n_R(1-n_L)], \tag{38}$$

where $\mathbb{N}_1(\omega)=\mathbb{B}_1/\mathbb{K}(\lambda=0)$ and $\mathbb{N}_2(\omega)=\mathbb{B}_2/\mathbb{K}(\lambda=0)$. In addition, at $T=0$ we have $(n_L(1-n_R))^i = n_L(1-n_R)$, $(n_R(1-n_L))^i = n_R(1-n_L)$, and $(n_L(1-n_R))^i(n_R(1-n_L))^j = 0$ (if $i,j\neq 0$). Assuming $\mu_L > \mu_R$, the generating function can be further simplified to

$$\ln\chi(\lambda)|_{T\to 0} = \frac{\mathcal{T}}{2}\int_{-\frac{eV}{2}}^{\frac{eV}{2}}\frac{d\omega}{2\pi}\ln\left(1+\frac{\mathcal{N}(\omega)}{\mathcal{D}(\omega)}\right), \tag{39}$$

where the functions are $\mathcal{N}(\omega)$ and $\mathcal{D}(\omega)$ are defined as

$$\mathcal{N}(\omega) = e^{-2i\lambda_R}\big\{8e^{i(\lambda_L+\lambda_R)}\Gamma_L\Gamma_R\big[\epsilon_d^2+(\Sigma_{\rm M}(\omega)-\omega)^2+(\Gamma_L-\Gamma_R)^2\big]+4\big(\Sigma_{\rm M}(\omega)^2+4e^{2i\lambda_L}\Gamma_L^2\big)\Gamma_R^2 - 4e^{2i\lambda_R}\big[(1-e^{2i\lambda_L})\Sigma_{\rm M}(\omega)^2\Gamma_L^2+2\Gamma_L^3\Gamma_R+\Sigma_{\rm M}(\omega)^2\Gamma_R^2+2\Gamma_L\Gamma_R\big(\epsilon_d^2+(\Sigma_{\rm M}(\omega)-\omega)^2+\Gamma_R^2\big)\big]\big\}, \tag{40}$$

$$\mathcal{D}(\omega) = \big[\epsilon_d^2+(2\Sigma_{\rm M}(\omega)-\omega)\omega\big]^2+(\Gamma_L+\Gamma_R)^2+(\Gamma_L+\Gamma_R)^2\big[2\big(\epsilon_d^2+2\Sigma_{\rm M}(\omega)^2-2\Sigma_{\rm M}(\omega)\omega+\omega^2\big)\big]. \tag{41}$$

Equation (77) is the main result of this section which allows one to compute cumulants as a function of various physical parameters. We now simplify the above expression in the limit $\delta = 0$ and small bias $eV \to 0$. We keep only the leading order terms in eV, and simply set $\omega = 0$ in the integrand.[1]

$$\left.\frac{\ln\chi}{M}\right|_{eV\to 0} = \ln\left(\frac{\Gamma_Le^{i\lambda_L}+\Gamma_Re^{-i\lambda_R}}{\Gamma_L+\Gamma_R}\right), \tag{42}$$

where $M = \mathcal{T}V/2\pi = \mathcal{T}Ve^2/h$ is the number of incoming particles during the waiting time. As mentioned above, the expression (79) only depends on the ratio of Γ_L/Γ_R, and is independent of many other microscopic parameters such as ϵ_d and κ. This universality is due to the finite density of states at zero energy induced by the Majorana leaking into the QD, and is a characteristic feature of topological superconductivity.

To get some insight we compute now currents through the left and right junctions. Using Eq. (3), one finds

$$I_L = \frac{e^2}{h}\frac{\Gamma_L}{\Gamma_R+\Gamma_L}V, \tag{43}$$

$$I_R = -\frac{e^2}{h}\frac{\Gamma_R}{\Gamma_R+\Gamma_L}V. \tag{44}$$

Clearly, when $\Gamma_L \neq \Gamma_R$, there is Andreev contribution to the current due to the presence of a grounded superconductor:

$$I_A = \frac{e^2}{h}\frac{\Gamma_R-\Gamma_L}{\Gamma_R+\Gamma_L}V. \tag{45}$$

One can notice that when $\Gamma_R = 0$, we recover the previous results [46] corresponding to a single lead coupled to a TSC. Indeed, given that the voltage drop between the left lead and TSC is $V/2$, linear differential conductance dI/dV is equal to the universal value of $2e^2/h$. Next, at the symmetric point $\Gamma_R = \Gamma_L$, Andreev current becomes zero, and linear differential conductance between right-left leads is $dI_L/dV = e^2/2h$ which is consistent with the previous work on QD coupled to an ungrounded TSC [42,45]. In addition, if we reverse the right lead voltage $V_R = -V/2 \to V/2$, the linear conductance is also equal to the universal value $2e^2/h$ which is expected based on the RG analysis [38,46].

We now discuss higher order cumulants $n > 1$. One can check that the expressions for the shot noise (as well as other higher order cumulants) through the left and right leads are the same in the $eV \to 0$ limit. Beyond the $eV \to 0$ limit, this relation only holds for the symmetric couplings $\Gamma_L = \Gamma_R$. Therefore, we set $\lambda_R = 0$ from now on and study current fluctuations through the left junction only. By expanding the CGF in terms of $e^{i\lambda_L}$, one finds

$$\chi(\lambda_L) = \left(\frac{\Gamma_R}{\Gamma_R+\Gamma_L}\right)^M\sum_{n=0}^{\infty}\binom{M}{n}\left(\frac{\Gamma_L}{\Gamma_R}\right)^n e^{in\lambda_L}. \tag{46}$$

[1]Note that limits $\delta \to 0$ and $\omega \to 0$ are noncommutative. Here we first set $\delta = 0$ and then take the limit $\omega \to 0$.

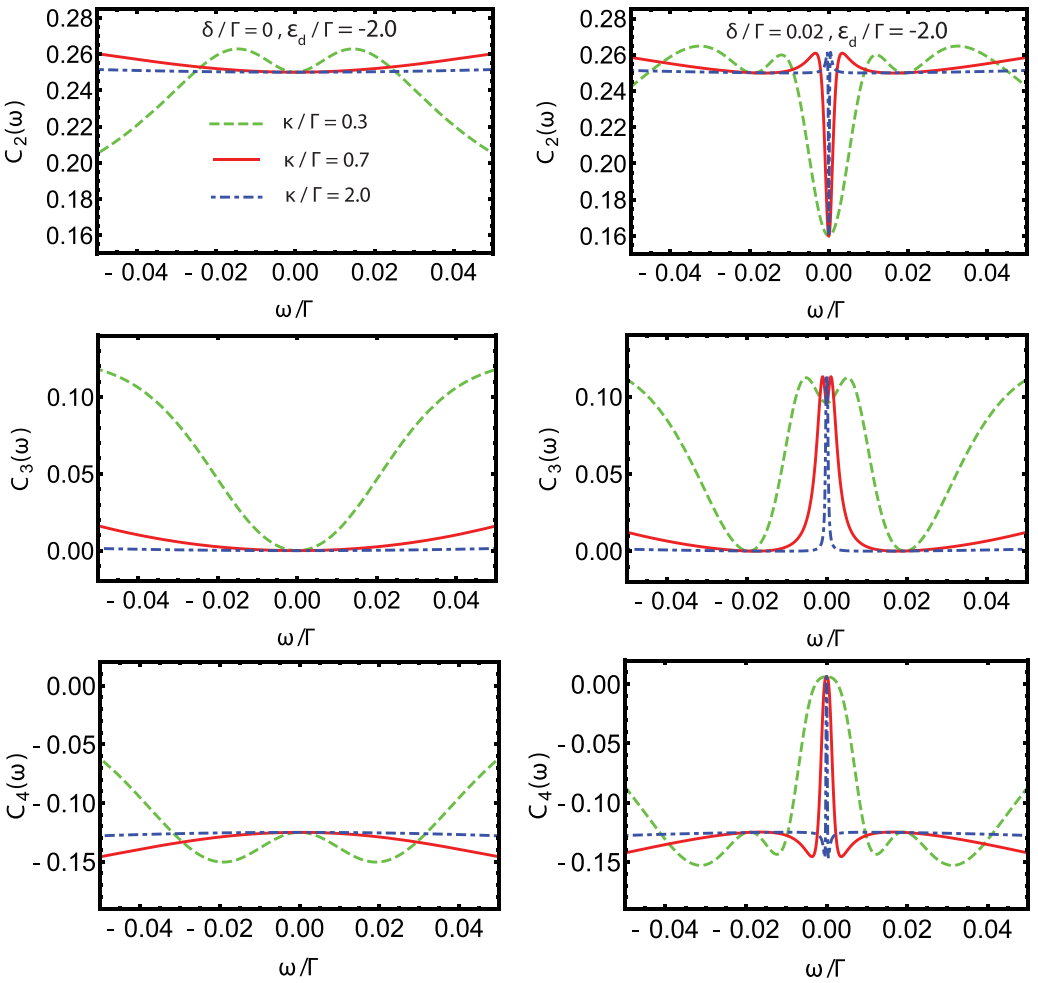

FIG. 2. (Color online) The cumulant spectrum $C_n(\omega)$ for $n = 2,3,4$ for different κ, $\delta = 0$ (left panel) and $\delta/\Gamma = 0.02$ (right panel). Here we set $\epsilon_d/\Gamma = -2.0$, $\Gamma_L = \Gamma_R$.

The probability $\mathcal{P}_q$ can be obtained by the Fourier transform,

$$\mathcal{P}_q = \frac{1}{2\pi}\int_0^{2\pi} d\lambda_L e^{-iq\lambda_L}\chi(\lambda_L) = \binom{M}{q}\left(\frac{\Gamma_R}{\Gamma_R+\Gamma_L}\right)^M\left(\frac{\Gamma_L}{\Gamma_R}\right)^q. \quad (47)$$

As expected, the generating function in the presence of MZM coupling $\kappa \neq 0$ is still described by the binomial distribution. However, the cumulants, defined as

$$C_n(0) = \frac{\langle\langle \delta^n q\rangle\rangle}{M} = (-i)^n \frac{1}{M}\frac{\partial^n}{\partial\lambda_L^n}\ln\chi(\lambda)\Big|_{\lambda_{L,R}=0}, \quad (48)$$

follow a peculiar pattern at $\Gamma_L = \Gamma_R$,

$$\{C_1(0)\cdots C_8(0)\} = \left\{\frac{1}{2},\frac{1}{4},0,-\frac{1}{8},0,\frac{1}{4},0,-\frac{17}{16}\right\},$$
$$C_n(0) = \frac{E_{n-1}(1)}{2}, \quad (49)$$

with $E_n(x)$ being the Euler polynomial. Contrary to the case without MZM, higher order cumulants are nonzero at $\Gamma_L = \Gamma_R$ and are independent of ϵ_d and κ.

The dependence of the cumulants on Majorana splitting energy δ and finite voltage bias (beyond linear in V contributions) can be obtained using Eq. (77). In this case, one needs to perform an integration of the cumulant spectrum $C_n(\omega)$ over $\omega \in (-eV/2, eV/2)$, where

$$C_n(\omega) = \frac{\langle\langle \delta^n q\rangle\rangle(\omega)}{M} = (-i)^n \frac{1}{2}\frac{\partial^n}{\partial\lambda_L^n}\ln\left(1+\frac{\mathcal{N}(\omega)}{\mathcal{D}(\omega)}\right)\Big|_{\lambda_{L,R}=0}. \quad (50)$$

The frequency dependence of the cumulants for $\epsilon_d/\Gamma = -2$ with different κ and δ are shown in Fig. 2 (left panel, $\delta = 0$; right panel, $\delta/\Gamma = 0.02$). As one can see, the cumulants exhibit plateaus corresponding to the universal values [see Eq. (49)] in the frequency range $\omega < \min\{\Gamma, \kappa^2/\Gamma\}$ which allows one to distinguish the Majorana physics from the other non-Majorana effects.

Next,we consider the effect of finite Majorana degeneracy splitting $\delta \neq 0$ which affects the cumulant spectrum $C_n(\omega)$ at small frequencies $\omega \to 0$. One can see that, provided $\kappa \gtrsim \Gamma$, the cumulants with $\delta = 0$ and $\delta \neq 0$ are similar for $|\omega| \gg \delta$.

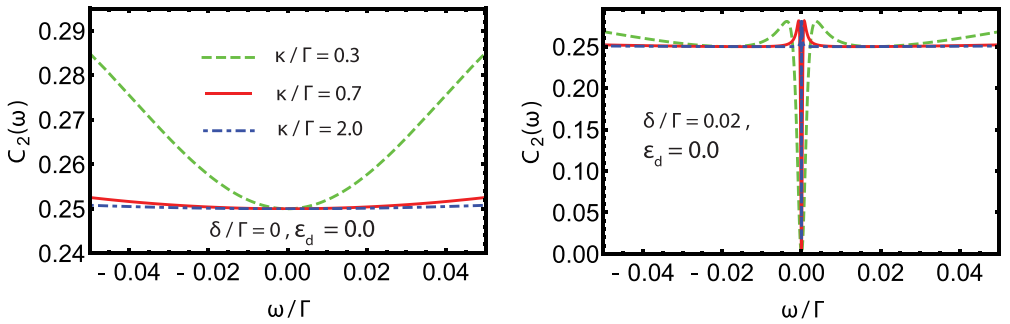

FIG. 3. (Color online) The $\epsilon_d = 0.0$ result of the second cumulant spectrum $C_2(\omega)$ for different κ, $\delta = 0$ (left panel) and $\delta/\Gamma = 0.02$ (right panel). Here we take $\Gamma_L = \Gamma_R$.

Therefore, in order to observe the universal values of C_ns, one has to adjust the source-drain bias V to the appropriate regime: $\min\{\kappa^2/\Gamma, \Gamma\} \gg eV \gg \delta$. One can notice that there is also a redistribution of the spectral weight for small κ/Γ. Therefore, the large $\kappa/\Gamma \gtrsim 1$ limit is more favorable for the experimental measurement of the cumulants.

Finally, we plot the second cumulant spectrum $C_2(\omega)$ for $\epsilon_d = 0$ in Fig. 3. We can see that although the quantitative value shows small changes compared to the $\epsilon_d/\Gamma = -2$ result, the conditions for the source-drain bias shown above still hold indicating that our results are robust against changes of ϵ_d.

IV. WEAKLY INTERACTING SPINFUL QD COUPLED TO A MZM

In this section, we consider the spinful model for a QD coupled to a MZM which is relevant in the context of the Majorana proposals involving topological insulators [9,10,15]. Indeed, MZM can be localized, for example, at the domain wall between an s-wave superconductor and a magnetic insulator of a quantum spin Hall insulator heterostructure. Assuming that the magnetic insulator, polarized along the z axis, does not affect the spin in QD (i.e., Zeeman splitting in QD is negligibly small), one arrives at the following effective Hamiltonian:

$$H_{\text{QD-MZM}} = \sum_\sigma \epsilon_d d_\sigma^\dagger d_\sigma + U d_\uparrow^\dagger d_\uparrow d_\downarrow^\dagger d_\downarrow + i\kappa(d_\uparrow + d_\uparrow^\dagger)\gamma_1 + i\delta\gamma_1\gamma_2. \quad (51)$$

Here we also include the effect of inter-particle interaction U assuming that it is weak, i.e., $U \ll \Gamma, \kappa$. The opposite limit of strong Coulomb interaction in the dot is considered in Sec. V.

As shown in the previous section, the CGF for spinless QD becomes universal (i.e., independent of ϵ_d and κ) due to the MZM coupling. In the spinful case, only one channel [e.g., spin-up) effectively couples to the MZM; see Eq. (51)]. Thus, the CGF will also have a nonuniversal contribution from the spin-down channel which is decoupled from MZM. However, as follows from Eq. (35), higher order cumulants (i.e., $n > 1$) from the spin-down channel vanish at $\epsilon_d = 0$ and $\Gamma_L = \Gamma_R$ enabling one to observe the universal part originating from the spin-up part. Thus, some fine tuning is necessary in this case (as opposed to the strongly interacting case in Sec. V). In addition to the aforementioned corrections to the universal features in FCS, one should also consider the effect of Coulomb interactions. Without loss of generality, we set $\lambda_R = 0$ and calculate effect interactions on charge fluctuations through the left lead. Our conclusions also apply to charge fluctuations through the right lead.

We now consider the effect of weak interactions $U \ll \{\Gamma, \kappa\}$ on FCS. We first calculate the contribution of the Coulomb interaction to the self-energy and then obtain the corrections to the CGF in powers of U. Up to the second order in U, the corresponding Feynman diagrams are shown in Fig. 4. The linear in U contribution to the self-energy $\Sigma_{d\bar{d}}^{\lambda_L}$ (see Fig. 4) merely represents the renormalization of the QD energy level ϵ_d. This is a trivial interaction effect which does not modify our previous conclusions. We, therefore, focus on U^2 contributions. The self-energy in the Nambu space has the following form,

$$\Sigma^{\lambda_L} = \begin{pmatrix} \Sigma_{d\bar{d}}^{\lambda_L} & \Sigma_{dd}^{\lambda_L} \\ \Sigma_{\bar{d}\bar{d}}^{\lambda_L} & \Sigma_{\bar{d}d}^{\lambda_L} \end{pmatrix}, \quad (52)$$

where $\Sigma_{\bar{d}d}^{\lambda_L}$ and $\Sigma_{\bar{d}\bar{d}}^{\lambda_L}$ are particle-hole conjugation of $\Sigma_{d\bar{d}}^{\lambda_L}$ and $\Sigma_{dd}^{\lambda_L}$. We note that all the Green's functions here depend on the counting field λ_L. The details of the calculation of Σ^{λ_L} is presented in Appendix B 1. After some manipulations, the cumulant generating function for each spin channel can be written as

$$\begin{aligned} \ln\chi(\lambda) &= \frac{\mathcal{T}}{2}\int_{-\infty}^{\infty}\frac{d\omega}{2\pi}\ln\frac{\det\left[\left[\check{Q}_{dd,U=0}^{\lambda_L}\right]^{-1} - \Sigma^{\lambda_L}\right]}{\det\left[\left[\check{Q}_{dd,U=0}^{\lambda_L=0}\right]^{-1} - \Sigma^{\lambda_L=0}\right]} \\ &= \frac{\mathcal{T}}{2}\int_{-\infty}^{\infty}\frac{d\omega}{2\pi}\ln\frac{\det\left[\left[\check{Q}_{dd,U=0}^{\lambda_L}\right]^{-1}\right]}{\det\left[\left[\check{Q}_{dd,U=0}^{\lambda_L=0}\right]^{-1}\right]} \\ &\quad + \frac{\mathcal{T}}{2}\int_{-\infty}^{\infty}\frac{d\omega}{2\pi}\ln\frac{\det\left[\mathbb{I}_{4\times4} - \check{Q}_{dd,U=0}^{\lambda_L}\Sigma^{\lambda_L}\right]}{\det\left[\mathbb{I}_{4\times4} - \check{Q}_{dd,U=0}^{\lambda_L=0}\Sigma^{\lambda_L=0}\right]}, \end{aligned} \quad (53)$$

where

$$\left[\check{Q}_{dd,U=0}^{\lambda_L}\right]^{-1} = \left[\check{Q}_{0,dd}^{\lambda_L}\right]^{-1} - \sum_\alpha\left(\sum_i M_{T,\alpha}^i\otimes\gamma^i\right)^\dagger\check{Q}_{0,\alpha} \times\left(\sum_i M_{T,\alpha}^i\otimes\gamma^i\right). \quad (54)$$

The first term in the generating function corresponds to the result for noninteracting case [see Eq. (30)], whereas the second term originates from the interaction-induced corrections.

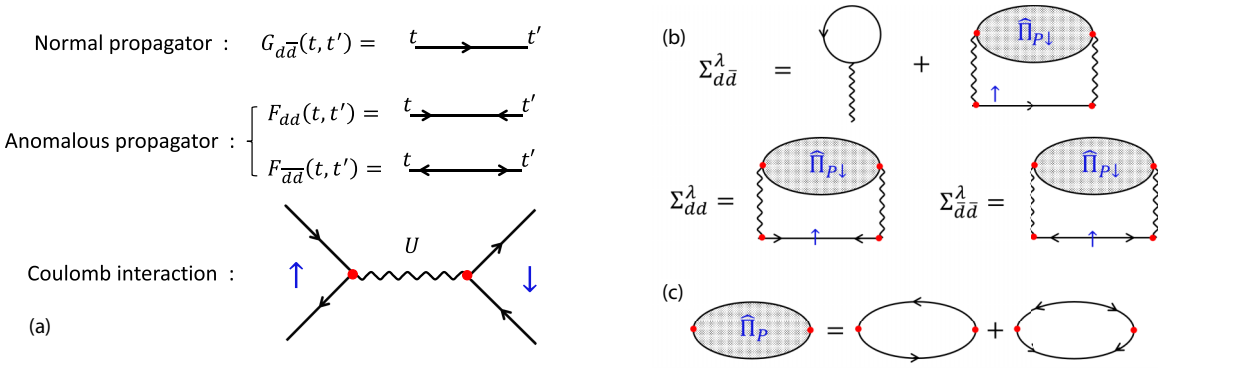

FIG. 4. (Color online) (a) Diagrammatic representation of the normal and anomalous impurity Green functions and the Coulomb interaction; (b) and (c) diagrammatic representation of the self-energy due to leading order corrections of the Coulomb interaction.

We consider weak Coulomb interactions $U \ll \{\Gamma,\lambda,eV\}$, and keep the leading order terms in U: $\breve{Q}^{\lambda_L}_{dd,U=0}\Sigma^{\lambda_L} \sim U^2/\min\{\Gamma,\lambda,eV\}^2 \ll 1$. By expanding the second term in Eq. (53) up to quadratic order in U, we obtain

$$\ln\chi(\lambda) \approx \frac{\mathcal{T}}{2}\int_{-\infty}^{\infty}\frac{d\omega}{2\pi}\ln\frac{\det\left[\left[\breve{Q}^{\lambda_L}_{dd,U=0}\right]^{-1}\right]}{\det\left[\left[\breve{Q}^{\lambda_L=0}_{dd,U=0}\right]^{-1}\right]} - \frac{\mathcal{T}}{2}\int_{-\infty}^{\infty}\frac{d\omega}{2\pi} \times\left[\mathrm{Tr}\left(\breve{Q}^{\lambda_L}_{\mathrm{dd,U=0}}\Sigma^{\lambda_L}\right) - \mathrm{Tr}\left(\breve{Q}^{\lambda_L=0}_{\mathrm{dd,U=0}}\Sigma^{\lambda_L=0}\right)\right], \quad (55)$$

where we used the relation $\det(\mathbb{I}+x\breve{A})\approx 1+x\mathrm{Tr}(\breve{A})$ for $x\ll 1$.

After some manipulations (see Appendix B 1), the cumulant generating function for small U can be written as

$$\ln\chi_\sigma(\lambda_L,U) \approx \ln\chi_\sigma(\lambda_L,U=0) - \frac{\mathcal{T}U^2}{2}\Xi^{\widetilde{K}}_{\lambda}, \quad (56)$$

which can be described by Fig. 5. Note that the matrix formalism of the Green functions has the form $\left(\begin{smallmatrix} G^R & G^K \\ G^{\widetilde{K}} & G^A\end{smallmatrix}\right)$ (i.e., with a L-O rotation). However, for the convenience of the calculation, we will also use the matrix Green functions in the Schwinger-Keldysh space (without L-O rotation). Here the function Ξ_λ [λ here means (λ_L,λ_R)] in the Schwinger-Keldysh space has the form,

$$\Xi_\lambda = \begin{pmatrix}\Xi^T_\lambda & \Xi^<_\lambda \\ \Xi^>_\lambda & \Xi^{\widetilde{T}}_\lambda\end{pmatrix}, \quad (57)$$

where

$$\Xi^T_\lambda = \int_{-\infty}^{\infty}\frac{d\Omega}{2\pi}\left(\hat{\Pi}^T_{P,\uparrow}(-\Omega)\hat{\Pi}^T_{P,\downarrow}(\Omega)+\hat{\Pi}^T_{H,\uparrow}(-\Omega)\hat{\Pi}^T_{H,\downarrow}(\Omega)\right),$$
$$\Xi^{\widetilde{T}}_\lambda = \int_{-\infty}^{\infty}\frac{d\Omega}{2\pi}\left(\hat{\Pi}^{\widetilde{T}}_{P,\uparrow}(-\Omega)\hat{\Pi}^{\widetilde{T}}_{P,\downarrow}(\Omega)+\hat{\Pi}^{\widetilde{T}}_{H,\uparrow}(-\Omega)\hat{\Pi}^{\widetilde{T}}_{H,\downarrow}(\Omega)\right),$$
$$\Xi^<_\lambda = \int_{-\infty}^{\infty}\frac{d\Omega}{2\pi}\left(\hat{\Pi}^<_{P,\uparrow}(-\Omega)\hat{\Pi}^<_{P,\downarrow}(\Omega)+\hat{\Pi}^<_{H,\uparrow}(-\Omega)\hat{\Pi}^<_{H,\downarrow}(\Omega)\right),$$
$$\Xi^>_\lambda = \int_{-\infty}^{\infty}\frac{d\Omega}{2\pi}\left(\hat{\Pi}^>_{P,\uparrow}(-\Omega)\hat{\Pi}^>_{P,\downarrow}(\Omega)+\hat{\Pi}^>_{H,\uparrow}(-\Omega)\hat{\Pi}^>_{H,\downarrow}(\Omega)\right), \quad (58)$$

and

$$\Xi^{\widetilde{K}}_\lambda = \left(\Xi^T_\lambda + \Xi^{\widetilde{T}}_\lambda - \Xi^<_\lambda - \Xi^>_\lambda\right)/2. \quad (59)$$

The polarization functions $\hat{\Pi}^\alpha_{P,\sigma}$ and $\hat{\Pi}^\alpha_{H,\sigma}$ (see Fig. 4) are calculated in Appendix B 1. One can notice that, for $\epsilon_d = 0$, the particle parts are exactly the same as the hole parts: $\hat{\Pi}_{P,\sigma} = \hat{\Pi}_{H,\sigma}$. Thus, the functions Ξ_λ for the spin-up channel have the same form as those for the spin-down channel, and we drop the spin index in Ξ_λ from now on. Lastly, it is well known that the function $\Xi^{\widetilde{K}}_{\lambda=0} = 0$ (here $\lambda = 0$ means $\lambda_L = \lambda_R = 0$) vanishes because of causality and unitarity. However, the presence of the artificial counting field $\lambda(t)$ having a different sign on the forward branch and backward branches of the Keldysh contour breaks unitarity. Therefore, the relation $\Xi^{\widetilde{K}}_{\lambda=0} = 0$ does not hold for $\lambda \neq 0$, and we have to evaluate it explicitly. In general, the calculation of $\Xi^{\widetilde{K}}_{\lambda,A}$ is not very illuminating but some simplification can be obtained by expanding the interaction-induced corrections in powers of eV assuming that $eV \to 0$. After some algebra (see Appendixes B 2, B 3, and B 4), we find that the leading contribution to CGF is proportional to V^3:

$$\Xi^{\widetilde{K}}_{\lambda,A} = (eV)^3\left(\Xi^{\widetilde{K},(3)}_{\lambda,A} + \Xi^{\widetilde{K},(3)}_{\lambda,B}\right), \quad (60)$$

where the functions $\Xi^{\widetilde{K},(3)}_{\lambda,A}$ and $\Xi^{\widetilde{K},(3)}_{\lambda,B}$ are given by

$$\Xi^{\widetilde{K},(3)}_{\lambda,A} = \frac{(e^{-i\lambda_L}-1)}{6\pi\Gamma^4}\mathbf{O}(\widetilde{\kappa}) + \left(2-\frac{\pi^2}{4}\right)\frac{(e^{i\lambda_L}-1)[(e^{i\lambda_L}-1)-2(e^{i\lambda_L}+3)\widetilde{\kappa}^2]}{12\pi^3(e^{i\lambda_L}+1)^2\Gamma^4\widetilde{\kappa}^2}, \quad (61)$$

$$\Xi^{\widetilde{K},(3)}_{\lambda,B} = \frac{1}{24\pi^3\Gamma^4\kappa^2(1+e^{i\lambda_L})^2}[15\kappa^2(e^{i\lambda_L}-1)+\kappa^2(e^{2i\lambda_L}-1)+(-2\Gamma^2-15\kappa^2)(e^{-i\lambda_L}-1)+(\Gamma^2-8\kappa^2)(e^{-2i\lambda_L}-1)] + \frac{\hat{\Pi}^T_{P2,\uparrow}(0^+,0)-\hat{\Pi}^{\widetilde{T}}_{P2,\uparrow}(0^+,0)}{6\pi^2\Gamma^3}(e^{-i\lambda_L}-1), \quad (62)$$

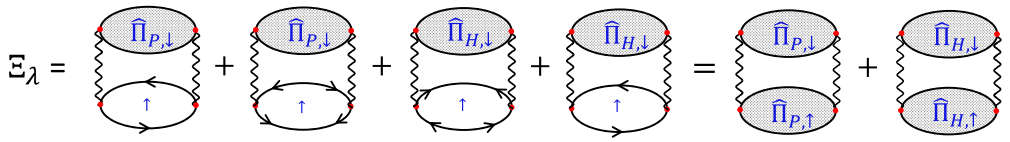

FIG. 5. (Color online) Diagrammatic representation of the cumulant generating function up to the leading order corrections of the Coulomb interaction.

where

$$\mathbf{O}(\widetilde{\kappa}) = \int_{-\infty}^{\infty} \frac{d\widetilde{\Omega}}{2\pi}\left[\hat{\Pi}^{T}_{P,\uparrow}(-\widetilde{\Omega},0)\frac{-i}{(|\widetilde{\Omega}|+i)^2} + \hat{\Pi}^{\widetilde{T}}_{P,\uparrow}(-\widetilde{\Omega},0)\frac{-i}{(|\widetilde{\Omega}|-i)^2}\right], \quad \text{with} \quad \widetilde{\Omega} = \frac{\Omega}{\Gamma}, \quad \widetilde{\kappa} = \frac{\kappa}{\Gamma}. \tag{63}$$

One can check that indeed the above expression vanishes for $\lambda_L = 0$, as required by unitarity. The integral in Eq. (61) is a dimensionless number depending only on κ/Γ. The functions $\hat{\Pi}^{T,\widetilde{T}}_{P2,\uparrow}(0^+,0)$ in Eq. (62) are defined in Eq. (B19); these functions depend on Γ and κ [89–92].[2]

Combining all the terms, the final expression for the cumulant generating function of the spinful QD at the $O(U^2)$ level can be written as

$$\ln\chi(\lambda_L,U) \approx \ln\chi_{\uparrow}(\lambda_L,U=0) + \ln\chi_{\downarrow}(\lambda_L,U=0) - \mathcal{T}U^2(eV)^3\left(\Xi^{\widetilde{K},(3)}_{\lambda,A} + \Xi^{\widetilde{K},(3)}_{\lambda,B}\right), \tag{64}$$

and the leading correction for the current and shot noise (for left junction current) can be written as

$$\delta I^{U}_{L} = \frac{e}{h}\frac{U^2(eV)^3}{\Gamma^4}\left(\frac{\mathbf{O}(\widetilde{\kappa})}{6\pi} + \left(2-\frac{\pi^2}{4}\right)\frac{1}{6\pi^3} - \frac{1}{2\pi^3} + \frac{\hat{\Pi}^{T}_{P2,\uparrow}(0^+,0) - \hat{\Pi}^{\widetilde{T}}_{P2,\uparrow}(0^+,0)}{6\pi^2}\right), \tag{65}$$

$$\delta S^{U}_{LL} = -\frac{e}{h}\frac{U^2(eV)^3}{\Gamma^4}\left(\frac{\mathbf{O}(\widetilde{\kappa})}{6\pi} + \left(2-\frac{\pi^2}{4}\right)\frac{1+2\widetilde{\kappa}^2}{24\pi^3\widetilde{\kappa}^2} + \frac{1-62\widetilde{\kappa}^2}{48\pi^3\widetilde{\kappa}^2} + \frac{\hat{\Pi}^{T}_{P2,\uparrow}(0^+,0) - \hat{\Pi}^{\widetilde{T}}_{P2,\uparrow}(0^+,0)}{6\pi^2}\right). \tag{66}$$

Thus, the leading order correction to the generating function in the presence of MZM coupling is of the order of $(eV)^3$ which is the same in the case without MZM considered in Ref. [68]. Since the leading order correction to the cumulants C_n is of the order of $(eV)^2$, the interaction-induced corrections do not affect cumulants at small bias. Therefore, we expect that one can observe the universal values of the cumulants discussed in Sec. III in realistic experimental conditions.

V. STRONGLY INTERACTING SPINFUL QD COUPLED TO A MAJORANA ZERO MODE: INTERPLAY OF KONDO AND MAJORANA COUPLINGS

In this section, we study another nontrivial case corresponding to a strongly interacting spinful QD in the limit of single-electron occupancy coupled to a MZM. The Hamiltonian for the system reads

$$H = H_{0\mathrm{L}} + H_{0\mathrm{R}} + H_{\text{QD-MZM}} + H_{\mathrm{T}}, \tag{67}$$

$$H_{\text{QD-MZM}} = \sum_{\sigma}\epsilon_d n_\sigma + U n_\uparrow n_\downarrow + i\kappa\gamma_1(d_\uparrow + d^{\dagger}_{\uparrow}) + i\delta\gamma_1\gamma_2. \tag{68}$$

[2]We note here that Eqs. (61) and (62) contain terms proportional to $(1+e^{i\lambda_L})^{-2}$ which can be represented as an infinite series in $e^{i\lambda_L}$. Similar terms in CGF also appear in other interacting systems [89–92], and there has been some debate as to their interpretation. We note, however, that physical observables (cumulants) are well defined even in the presence of these terms; cf. Eq. (65).

$$H_{\mathrm{T}} = \sum_{\alpha=L,R,\sigma}(t_\alpha\psi^{\dagger}_{\alpha,\sigma}(0)d_\sigma + \text{H.c.}). \tag{69}$$

Here $H_{0\mathrm{R}}$ and $H_{0\mathrm{L}}$ correspond to the right and left noninteracting lead, respectively; $d^{\dagger}_{\sigma}$ and d_σ are electron creation and annihilation operators in the QD with $n_\sigma = d^{\dagger}_{\sigma}d_\sigma$; the energies ϵ_d and U correspond to the QD energy level and the on-site repulsive interaction. κ and δ represent coupling between QD electrons and MZM and the degeneracy splitting energy in TSC. The operator $\psi^{\dagger}_{\alpha,\sigma}(0)$ corresponds to an electron annihilation operator in the lead α with spin σ at the junction with the QD (i.e., $x=0$) and t_α is the corresponding amplitude for tunneling. Once again, we assume here that Zeeman splitting in a QD is negligibly small [see discussion after Eq. (51). In the limit of single-electron occupancy (i.e., large U and $\epsilon_d < 0$), considered henceforth, one has to take into account interplay of Kondo and Majorana couplings [46]. In the next subsections, we present calculations for the FCS of charge fluctuations using two different techniques: exact solution at the particle-hole symmetric point and slave-boson approximation, both of which show that the zero-frequency cumulants calculated in the linear response regime exhibit a universal pattern described by Euler polynomial.

A. Low-energy effective theory at the particle hole symmetric point

In this section, we study FCS of charge fluctuations at the particle-hole symmetric point where one can solve the problem

exactly; see Ref. [46]. First, in the limit of a large charging energy, one can project out double-electron occupancy state in the QD using Schrieffer-Wolff transformation [46]. The effective low-energy Hamiltonian at the particle-hole symmetric point ($\epsilon_d = -U/2$) reads

$$H_{\rm eff} = H_{0L} + H_{0R} + \sum_{j=x,y,z;\alpha=R,L} i J_{2\alpha}\gamma_1 S_j \Phi_{j\alpha}(0) + \sum_{\alpha\alpha'=L,R} J_{3,\alpha\alpha'}\vec{\mathbf{S}}\cdot\vec{\mathbf{s}}_{\alpha\alpha'}(0), \tag{70}$$

where $\vec{\mathbf{S}} = \{S_x, S_y, S_z\}$ are spin operators for the dot, and γ_1 is the Majorana zero mode at the end of the TSC wire. We also define the Majorana operators from the lead fermions: $\Phi_{\alpha,x}(0) = \psi_{\alpha\downarrow}(0) + \psi^\dagger_{\alpha\downarrow}(0)$, $\Phi_{\alpha,y}(0) = i(-\psi_{\alpha\downarrow}(0) + \psi^\dagger_{\alpha\downarrow}(0))$, and $\Phi_{\alpha,z}(0) = \psi_{\alpha\uparrow}(0) + \psi^\dagger_{\alpha\uparrow}(0)$. The lead spin operator is defined as $\vec{\mathbf{s}}_{\alpha\alpha'}(0) = \psi^\dagger_{\alpha s}(0)(\vec{\sigma}/2)^{ss'}\psi_{\alpha' s'}(0)$. The coupling constants $J_{2\alpha}$ and $J_{3\alpha\alpha'}$ are given by

$$J_{2\alpha} = \eta|t_\alpha|\left(\frac{1}{|\epsilon_d|} + \frac{1}{U-|\epsilon_d|}\right), \qquad J_{3\alpha\alpha'} = |t_\alpha t_{\alpha'}|\left(\frac{1}{|\epsilon_d|} + \frac{1}{U-|\epsilon_d|}\right). \tag{71}$$

It has been shown in Ref. [46] that the low-energy fixed point corresponding to the Hamiltonian (70) is governed by the J_2 coupling which is the leading relevant perturbation in the model. It has been confirmed by the DMRG calculation [46] that the strong coupling fixed point corresponds to the nontrivial boundary conditions for the lead fermions—Andreev boundary conditions (BCs) for spin-up electrons and normal BCs for spin-down electrons. Some insight regarding the strong coupling fixed point can be obtained by setting $J_3 = 0$ and using the exact solution of the model [46]. The effect of the marginal perturbation J_3 can be taken into account perturbatively.

1. FCS using the exact solution of the model at $J_3 = 0$

The low-energy Hamiltonian (70) with $J_3 = 0$ can be further simplified by noticing that the operators $\zeta_j = 2\gamma_1 S_j$ ($j = x,y,z$) along with γ_2 satisfy the Clifford algebra and define the new Majorana operators $\zeta_j = 2\gamma_1 S_j$, which maps the model to the following fermion bilinear Hamiltonian [46]:

$$H_{\rm eff} = H_{0L} + H_{0R} + iJ_{2L}\sum_{j=x,y,z}\zeta_j\Phi_{Lj}(0) + iJ_{2R}\sum_{j=x,y,z}\zeta_j\Phi_{Rj}(0). \tag{72}$$

In order to study FCS for this model, we introduce the counting field λ_α by replacing $\psi^\dagger_{\alpha\sigma}(0)$ with $e^{-i\lambda_\alpha(t)/2}\psi^\dagger_{\alpha\sigma}(0)$, and then perform the Gaussian integration over fermionic fields:

$$\ln\chi(\lambda) = \frac{\mathcal{T}}{2}\int_{-\infty}^{\infty}\frac{d\omega}{2\pi}\ln\left[\frac{\det[\omega\check{\mathbb{I}}_{3\times3} - \check{Q}_{\Gamma\lambda}]}{\det[\omega\check{\mathbb{I}}_{3\times3} - \check{Q}_{\Gamma0}]}\right], \tag{73}$$

where the matrix is defined as $\check{Q}_{\Gamma\lambda}$:

$$\check{Q}_{\Gamma\lambda} = \sum_{\alpha=L,R} W^\dagger_{T,\alpha}\check{Q}_{0,\alpha}W_{T,\alpha}. \tag{74}$$

Here the Green function and the coupling matrix $\hat{W}_{T,\alpha}$ operate in the Keldysh-Nambu space. The Green function for the α lead $\check{Q}_{0,\alpha}$ is defined as

$$\check{Q}_{0,\alpha}(\omega) = \begin{pmatrix} g^0_{\alpha\uparrow}(\omega) & 0 & 0 & 0 \\ 0 & g^0_{\alpha\downarrow}(\omega) & 0 & 0 \\ 0 & 0 & \widetilde{g}^0_{\alpha\uparrow}(\omega) & 0 \\ 0 & 0 & 0 & \widetilde{g}^0_{\alpha\downarrow}(\omega) \end{pmatrix}, \tag{75}$$

where $g^0_{\alpha\sigma}(\omega)$ and $\widetilde{g}^0_{\alpha\sigma}(\omega)$ are given in Eqs. (20) and (21). The matrix $\hat{W}_{T,\alpha}$ describes the coupling between Majorana modes $\{\zeta_x,\zeta_y,\zeta_z\}$ and the lead electrons $\{\psi_{\alpha\uparrow},\psi_{\alpha\downarrow},\psi^\dagger_{\alpha\uparrow},\psi^\dagger_{\alpha\downarrow}\}$ at $x = 0$:

$$\hat{W}_{T,\alpha} = \begin{pmatrix} 0 & iJ_{2\alpha}m_{\lambda\alpha} & 0 & iJ_{2\alpha}\widetilde{m}_{\lambda\alpha} \\ 0 & J_{2\alpha}m_{\lambda\alpha} & 0 & -J_{2\alpha}\widetilde{m}_{\lambda\alpha} \\ iJ_{2\alpha}m_{\lambda\alpha} & 0 & iJ_{2\alpha}\widetilde{m}_{\lambda\alpha} & 0 \end{pmatrix}. \tag{76}$$

The matrices $m_{\lambda\alpha} = \cos(\lambda_\alpha)\mathbb{I} - i\sin(\lambda_\alpha)\sigma_x$ and $\widetilde{m}_{\lambda\alpha} = -\cos(\lambda_\alpha)\mathbb{I} - i\sin(\lambda_\alpha)\sigma_x$ are defined in Keldysh space. Note that in order to obtain the above expression for the matrix $\hat{W}_{T,\alpha}$, we used the relation $\lambda^{(1)}_\alpha = -\lambda^{(2)}_\alpha = \lambda_\alpha$ and applied the Larkin-Ovchinnikov rotation [87]. Assuming symmetric applied voltage bias $V_L = V/2$ and $V_R = -V/2$ (see Fig. 1), we find the generating function for this low-energy model at zero temperature $T = 0$:

$$\ln\chi(\lambda)|_{T\to0} = \frac{\mathcal{T}}{2}\int_{-\frac{eV}{2}}^{\frac{eV}{2}}\frac{d\omega}{2\pi}\ln\left(1 + \frac{\mathcal{N}(\omega)}{\mathcal{D}(\omega)}\right), \tag{77}$$

where the functions are $\mathcal{N}(\omega)$ and $\mathcal{D}(\omega)$ are

$$\begin{aligned}\mathcal{N}(\omega) = {} & -(4(\Gamma_{2L}+\Gamma_{2R})^2+\omega^2)^3 + e^{-4i\lambda_R}(e^{i\lambda_R}(4(\Gamma_{2L}-\Gamma_{2R})^2+\omega^2) \\ & + 16\Gamma_{2L}e^{i\lambda_L}\Gamma_{2R})^2\left(e^{2i\lambda_R}\left(\omega^2+4\Gamma^2_{2L}e^{2i\lambda_L}\right) + 8\Gamma_{2L}\Gamma_{2R}e^{i(\lambda_L+\lambda_R)} + 4\Gamma^2_{2R}\right), \\ \mathcal{D}(\omega) = {} & (4(\Gamma_{2L}+\Gamma_{2R})^2+\omega^2)^3.\end{aligned} \tag{78}$$

In the linear response regime, we arrive at the following generating function:

$$\left.\frac{\ln\chi}{M}\right|_{eV\to0} = \ln\left(\frac{(\Gamma_{2L}e^{i\lambda_L} + \Gamma_{2R}e^{-i\lambda_R})((\Gamma_{2L}-\Gamma_{2R})^2 + 4e^{i(\lambda_L-\Lambda_R)}\Gamma_{2L}\Gamma_{2R})}{(\Gamma_{2L}+\Gamma_{2R})^3}\right), \tag{79}$$

where $\Gamma_{2\alpha} = \pi\rho_F J_{2\alpha}^2$ and $M = \mathcal{T}V/2\pi = \mathcal{T}Ve^2/h$ has the meaning of the number of incoming particles during the waiting time. The cumulants of the current fluctuations through the left-lead junction are given by

$$C_n(0) = (-i)^n \frac{1}{M}\frac{\partial^n}{\partial\lambda_L^n}\ln\chi(\lambda)\Big|_{\lambda_{L,R}=0}. \tag{80}$$

For the symmetric left-right lead couplings $J_{2L} = J_{2R}$, the cumulants follow a peculiar universal pattern,

$$\{C_1(0)\cdots C_8(0)\} = \left\{\frac{3}{2},\frac{1}{4},0,-\frac{1}{8},0,\frac{1}{4},0,-\frac{17}{16}\right\},$$
$$C_n(0) = \frac{E_{n-1}(1)}{2} \quad \text{for } n \geqslant 2, \tag{81}$$

with $E_n(x)$ being the Euler polynomial.

2. *Corrections to FCS due to finite Kondo coupling $J_3 \neq 0$*

In this subsection we consider the effect of the Kondo coupling and show that its contribution to FCS is higher order in applied voltage bias eV. We first provide qualitative arguments based on the RG equations and then corroborate our conclusions using the perturbative calculation in J_3. The perturbative RG analysis [46] shows that J_2 coupling is the leading relevant perturbation in the model which flows to strong coupling and changes the boundary conditions for the conduction electrons. At the strong coupling fixed point, the Majorana operators ζ_j are effectively absorbed by the conduction electrons in the leads—spin-up electrons absorb a Majorana mode whereas spin-down electrons absorb a Dirac fermion mode which leads to new boundary conditions: Andreev BCs for spin-up electrons and normal BCs (Kondo) for spin-down electrons: $A_\uparrow \otimes N_\downarrow$. Next, we rewrite the QD impurity spin in terms of the Majorana operators ζ_j:

$$S_i = -2i\varepsilon_{ijk}S_jS_k = -\frac{i}{2}\varepsilon_{abc}\zeta_j\zeta_k. \tag{82}$$

Thus, the Kondo Hamiltonian written in terms of the new operators ζ_j reads

$$H_K = -\frac{i}{2}\sum_{\alpha\alpha'=L,R} J_{3,\alpha\alpha'}(\zeta_y\zeta_z s_{x,\alpha\alpha'}(0) + \zeta_z\zeta_x s_{y,\alpha\alpha'}(0) + \zeta_x\zeta_y s_{z,\alpha\alpha'}(0)). \tag{83}$$

Since Majorana operators are now effectively absorbed by the conduction electrons, the scaling dimension of the Kondo term has changed. Indeed, the Kondo coupling written in the new variables looks like the four-fermion interaction term. Therefore, the RG flow for the Kondo coupling J_3 at the strong coupling fixed point is given by

$$\frac{dJ_3}{dl} = -J_3, \tag{84}$$

and, thus, the Kondo term becomes an irrelevant perturbation. Therefore, the second order in J_3 contribution to the shot noise (as well as other cumulants) is proportional to $(eV)^2$, and is vanishing in the linear response regime. This conclusion is in complete agreement with the previous results in Sec. IV where we showed that the contribution to FCS of the Kondo term is proportional to $(eV)^3$. Following exactly the same procedure as

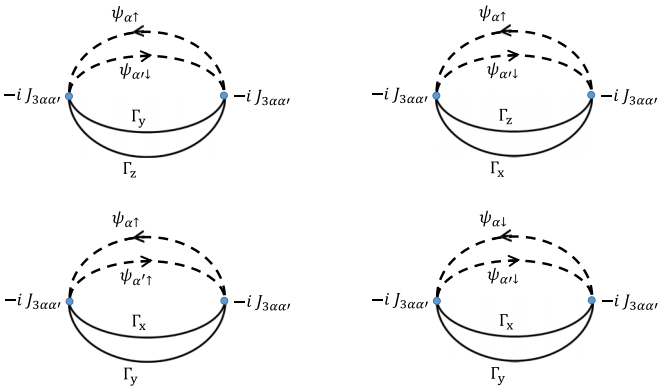

FIG. 6. (Color online) Diagrammatic representation of the cumulant generating function up to the leading order corrections of the J_3. The solid lines describe the Majorana propagators, and the dashed lines describe the propagators of the free electron in the leads.

Sec. IV [refer to Eqs. (52)–(56)], we now calculate the leading order correction in J_3 coupling to the generating function:

$$\ln\chi_\sigma(\lambda_L, J_3) \approx \ln\chi_\sigma(\lambda_L, J_3 = 0) - \sum_{\alpha\alpha'}\frac{\mathcal{T}J_{3\alpha\alpha'}^2}{2}\Xi^{\tilde{K}}_{\alpha\alpha',\lambda}. \tag{85}$$

The Feynman diagrams corresponding to the second-order correction in J_3 to the free energy are shown in Fig. 6. Following the procedure outlined in Sec. IV and Appendix B, we first expand the CGF in powers of eV and calculate the lowest nonvanishing contribution. After some algebra, one finds that the leading order correction to the CGF is proportional to $(eV)^3$:

$$\Xi^{\tilde{K}}_{LR,\lambda} = -\frac{5(eV)^3\rho_F^2}{12\pi^3\Gamma_2^2}e^{-2i\lambda_L}\cos^2\lambda_L + O(eV^4), \tag{86}$$
$$\Xi^{\tilde{K}}_{RL,\lambda} = \frac{(eV)^3\rho_F^2}{12\pi^3\Gamma_2^2}e^{2i\lambda_L}\cos^2\lambda_L + O(eV^4), \tag{87}$$
$$\Xi^{\tilde{K}}_{LL,\lambda} = -\frac{(eV)^3\rho_F^2}{12\pi^3\Gamma_2^2}\cos(2\lambda_L)\cos^2\lambda_L + O(eV^4), \tag{88}$$
$$\Xi^{\tilde{K}}_{RR,\lambda} = -\frac{(eV)^3\rho_F^2}{12\pi^3\Gamma_2^2}\cos(2\lambda_L)\cos^2\lambda_L + O(eV^4). \tag{89}$$

Here ρ_F is the electron density of state at the Fermi level in the leads, and the coupling Γ_2 is defined as $\Gamma_2^2 = \pi J_2^2\rho_F$ (we consider $J_{2L} = J_{2R} = J_2$).

At the end of the day, we find that our prediction regarding the universal FCS of current fluctuations is not modified in the linear response regime since the contribution of the terms proportional to J_3 is higher order in voltage and, thus, can be neglected. Indeed, this universal sequence is completely determined by the properties of the fixed point itself rather than the fluctuations around it. This is to be contrasted with the Kondo fixed point where the shot noise and higher order cumulants are proportional to $(eV)^3$ [93] and, thus, depend on the details of irrelevant perturbations around the strong coupling fixed point.

B. FCS away from particle-hole symmetric point: Slave-boson mean-field theory

In this section, we provide a different perspective on the problem and consider current fluctuations in the QD-TSC system away from the particle-hole symmetric point. In the limit of single-electron occupancy $\{\Gamma,\kappa\} \ll |\epsilon_d| \ll U$, one can study the problem, defined by the Hamiltonian (67), using a slave-boson mean-field (SBMF) approximation originally developed for an infinite-U Anderson model [94,95]. This approach allows one to eliminate double occupancy in the QD and significantly simplify the problem. For the sake of completeness, we outline here main steps of the SBMF approach. We refer a reader to Ref. [46] for more details of the SBMF calculation in the presence of MZM. We first rewrite fermion operators in QD in terms of the auxiliary boson b and fermion f_σ operators, i.e., $d_\sigma \to f_\sigma b^\dagger$. This procedure requires one to introduce a constraint $b^\dagger b + \sum_\sigma f_\sigma^\dagger f_\sigma = 1$ on the Hilbert space. After the transformation, the effective Hamiltonian becomes

$$H_{\rm SBMF} = H_{\rm Leads} + \sum_\sigma \epsilon_d f_\sigma^\dagger f_\sigma + i\kappa\gamma_1(f_\uparrow b^\dagger + f_\uparrow^\dagger b) + \sum_{\alpha=L,R}\sum_\sigma t_\alpha(\psi_{\sigma,\alpha}^\dagger(0) f_\sigma b^\dagger + h.c.) + i\delta\gamma_1\gamma_2, \tag{90}$$

where the lead Hamiltonian $H_{\rm Leads}$ is unchanged. Next, we apply the mean-field approximation and replace the bosonic operator b and the Lagrangian multiplier η enforcing the constraint by their mean-field expectation values. We choose $\langle b\rangle = \langle b^\dagger\rangle = b$ to be a real positive number. The mean-field parameter b and η can be determined self-consistently by minimizing the free energy [46]:

$$b^2 + \sum_\sigma \langle f_\sigma^\dagger f_\sigma\rangle = 1, \tag{91}$$

$$2b\eta + t\sum_{\alpha=L,R}\sum_\sigma(\langle f_\sigma^\dagger \psi_{\sigma,\alpha}(0)\rangle + \text{c.c.}) + i\kappa\langle\gamma_1(f_\uparrow^\dagger + f_\uparrow)\rangle = 0. \tag{92}$$

Here, we assume the $eV \ll \max\{T_K,\kappa\}$ and thus neglect the dependence on voltage bias eV in the SMBF calculations; see also discussion in Ref. [96]. The above equations determine thermodynamics of the system, and we are now ready to compute transport properties. Once the mean-field values of the auxiliary parameters are determined in the SBMF approximation, spin-up and spin-down channels become decoupled. Thus, effectively the problem reduces to the previous model—spin-up channel is coupled to an MZM whereas the spin-down channel is not. The chemical potential and couplings are renormalized: $\epsilon_d \to \widetilde{\epsilon}_d = \epsilon_d + \eta$, $t_\alpha \to \widetilde{t}_\alpha = bt_\alpha$, $\Gamma_\alpha \to \widetilde{\Gamma}_\alpha = b^2\Gamma_\alpha$, and $\kappa \to \widetilde{\kappa} = b\kappa$.

Using the results of Sec. III, it is rather straightforward to obtain the CGF at small voltage bias $eV \to 0$ in this case,

$$\left.\frac{\ln\chi_{\rm KM}}{M}\right|_{eV\to 0} = \ln\left(\frac{\widetilde{\Gamma}_L e^{i\lambda_L} + \widetilde{\Gamma}_R e^{-i\lambda_R}}{\widetilde{\Gamma}_L + \widetilde{\Gamma}_R}\right) + \ln\left(1 + \frac{4\widetilde{\Gamma}_L\widetilde{\Gamma}_R}{\widetilde{\epsilon}_d^2 + (\widetilde{\Gamma}_L + \widetilde{\Gamma}_R)^2}(e^{i(\lambda_L-\lambda_R)} - 1)\right). \tag{93}$$

Here the first and second terms correspond to the spin-up and spin-down channels, respectively. As discussed below, the renormalized QD energy $\widetilde{\epsilon}_d$ is close to the Fermi level, i.e., $\widetilde{\epsilon}_d \to 0$, for a large parameter range $\{\kappa,\Gamma\} < |\epsilon_d|$ (so-called

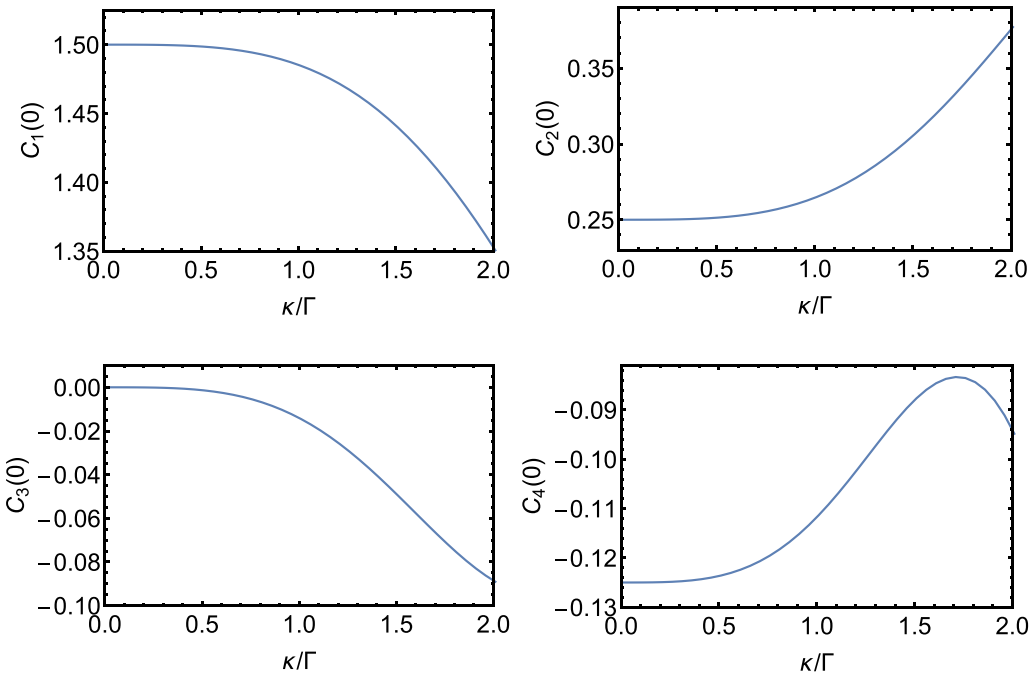

FIG. 7. (Color online) Dependence of the cumulants $C_n(0) = \langle\langle\delta^n q\rangle\rangle/M$ ($\delta = 0$ and $eV \to 0$ limit) on the Majorana coupling κ in the Kondo regime from SBMF calculation. We choose $\Gamma_L = \Gamma_R$, $\epsilon_d/\Gamma = -10.0$, and bandwidth $\Lambda/\Gamma = 30.0$.

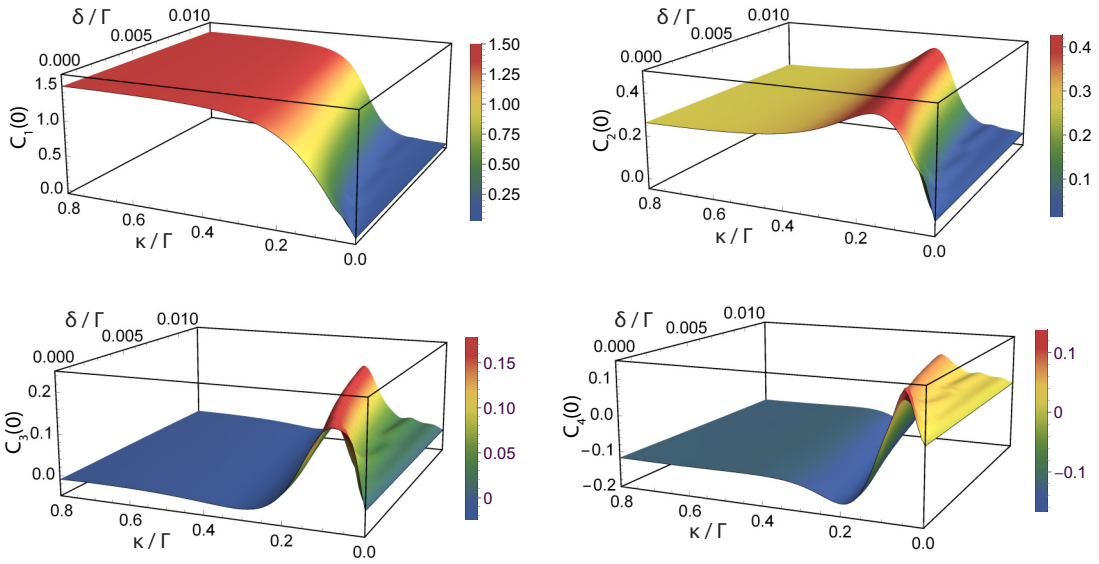

FIG. 8. (Color online) The cumulants $C_n(0)$ for $n = 1,2,3,4$ as a function κ and δ. Here $\epsilon_d/\Gamma = -10.0$, $\Gamma_L = \Gamma_R$, $eV/\Gamma = 0.001$, and $\Lambda/\Gamma = 30.0$.

universal limit). Thus, in the case of symmetric right-left lead couplings $\Gamma_R = \Gamma_L$, the second term in Eq. (79) is simply given by $i(\lambda_L - \lambda_R)$ and, therefore, does not contribute beyond the first cumulant. Thus, the shot noise as well as other higher order cumulants are once again given by the universal pattern:

$$\{C_1(0)\cdots C_8(0)\} = \left\{\frac{3}{2},\frac{1}{4},0,-\frac{1}{8},0,\frac{1}{4},0,-\frac{17}{16}\right\},$$
$$C_n(0) = \frac{E_{n-1}(1)}{2} \quad \text{for } n > 1, \tag{94}$$

with $E_n(x)$ being the Euler polynomial. Note that this result agrees perfectly with the FCS calculation at the particle-hole symmetric point; cf. Eq. (49). One may wonder here whether fluctuation corrections around the mean-field solution modify the universal pattern predicted for FCS of current fluctuations. This is an important question which is outside the scope of this paper but it is certainly encouraging that the SBMF theory agrees well with the exact solution obtained at the particle-hole symmetric point.

C. Results and discussion

The SBMF solution discussed above allows one to analyze different perturbations in more details. We begin with the case of zero degeneracy splitting $\delta = 0$ and study the dependence of the cumulants on the MZM coupling κ. In the linear response regime, the dependence of the cumulants on κ can be obtained numerically and is shown in Fig. 7. A recent study based on the SBMF approach [46] shows that there is a crossover between Kondo- and Majorana-dominated regimes as a function of the MZM coupling κ. For $\kappa \ll \kappa_c \equiv \sqrt{T_K/\Gamma}|\epsilon_d|$, the mean-field solution is determined by the Kondo temperature T_K:

$$\tilde{\Gamma} \equiv \Gamma b^2 = T_K \equiv \Lambda \exp(-\pi|\epsilon_d|/2\Gamma), \tag{95}$$

and the renormalized energy level is $\tilde{\epsilon}_d \equiv |\epsilon_d + \eta| \sim \Gamma b^4$. Here Λ is the bandwidth and $\Gamma = \Gamma_R + \Gamma_L$. Since $b \ll 1$, the renormalized energy $\tilde{\epsilon}_d$ is small $\tilde{\epsilon}_d \ll \tilde{\Gamma}$ [46]. Thus, the cumulants at exactly zero frequency and $\Gamma_R = \Gamma_L$ are given by Eq. (94). At finite temperature, there will be corrections to the universal values which are governed by Kondo temperature T_K. In the case of intermediate MZM coupling $\kappa \gg \kappa_c$, the parameter $b \sim \kappa/|\epsilon_d|$ is determined by the Majorana coupling. Therefore, the finite-temperature corrections to the universal values of the cumulants are determined by the Majorana coupling rather than the Kondo temperature.

Next we consider the effect of a finite energy splitting $\delta \neq 0$ and voltage bias on our prediction, which is important for the experimental detection in realistic settings. The cumulants $C_n(0)$ for $n = 1,2,3,4$ as a function κ and δ are shown in Fig. 8, where we focus on the limit $|\epsilon_d| \gg \{\Gamma,\kappa\}$. One can see that in order to resolve the universal quantized values, one has to adjust the voltage bias in the following range $\min\{\kappa^2/\Gamma,\Gamma b^2\} \gg eV \gg \delta$ where $b = \sqrt{T_K/\Gamma}$ for $\kappa \ll \kappa_c$ and $b = \kappa/|\epsilon_d|$ for $\kappa_c \ll \kappa \ll |\epsilon_d|$. The plot of the cumulant power spectra as a function of the splitting δ and Majorana coupling κ is shown in Fig. 8. One can notice that the width of the plateau around the quantized values gradually shrinks with increasing δ.

VI. CONCLUSIONS

In this paper, we study the full counting statistics of current fluctuations in a QD device with a side-coupled TSC; see Fig. 1. Two normal-metal leads, coupled to a QD, are also introduced in order to detect electric current fluctuations. Using the Keldysh path-integral approach, we compute the cumulant generating function for the QD with MZM coupling in this two-lead structure. We first consider a noninteracting spinless system, and find that for the symmetric left-right lead couplings $\Gamma_L = \Gamma_R$, the zero-frequency cumulants exhibit a universal pattern described by a series of numbers generated by the Euler polynomial. We show that the cumulants depend only on one dimensionless parameter Γ_L/Γ_R, and are independent of other microscopic parameters of the QD (i.e., QD energy level and QD-MZM coupling). We then

consider another realistic setup—a spinful QD coupled to a topological superconductor—and show that our prediction for the universal pattern in FCS of current fluctuations holds there as well. We consider the effect of Kondo couplings in the QD as well as other irrelevant perturbations and show that their contribution to the FCS is higher order in applied voltage bias, and, as such, can be neglected in the linear response regime. Our results provide a complete tool set for detecting Majorana modes in tunneling transport measurements which goes far beyond the zero-bias tunneling conductance paradigm.

ACKNOWLEDGMENTS

The work of A.L. was supported by NSF Grant No. ECCS-1407875. R.L. wishes to acknowledge the hospitality of the Aspen Center for Physics and support under NSF Grant No. 1066293. Support for this research at the University of Wisconsin-Madison was provided by the Office of the Vice Chancellor for Research and Graduate Education with funding from the Wisconsin Alumni Research Foundation.

APPENDIX A: DERIVATION OF THE COEFFICIENTS IN CGF EQ. (37)

In this Appendix, we provide details of the calculations of FCS for the noninteracting case. To evaluate the generating function, we first define

$$\mathbb{K}(\lambda_L,\lambda_R)=\det\left[\mathbb{I}_{4\times4}-\check{Q}_{0,dd}\sum_{\alpha}\left(\sum_i M^i_{T,\alpha}\otimes\gamma^i\right)^{\dagger}\check{Q}_{0,\alpha}\left(\sum_i M^i_{T,\alpha}\otimes\gamma^i\right)\right]. \tag{A1}$$

We consider a symmetric source-drain bias ($\mu_L=eV/2$ and $\mu_R=-eV/2$), and insert Eqs. (19), (22), and (27), (28) into $\mathbb{K}(\lambda_L,\lambda_R)$, and obtain

$$\begin{aligned}\mathbb{K}(\lambda_L=0,\lambda_R=0)=1+(\Gamma_L+\Gamma_R)^2\big(\big[G^R_{0,\bar{d}d}\big]^2+(\Gamma_L+\Gamma_R)^2\big[F^R_{0,dd}\big]^4-2\big[F^R_{0,dd}\big]^2\big(-1+(\Gamma_L+\Gamma_R)^2G^R_{0,d\bar{d}}G^R_{0,\bar{d}d}\big)\\+\big[G^R_{0,d\bar{d}}\big]^2\big(1+(\Gamma_L+\Gamma_R)^2\big[G^R_{0,\bar{d}d}\big]^2\big)\big),\end{aligned} \tag{A2}$$

and

$$\begin{aligned}\mathbb{K}(\lambda_L,\lambda_R)=\mathbb{K}(0,0)-\mathbb{C}_1n_L(1-n_L)-\mathbb{C}_2n_R(1-n_R)+\mathbb{B}_1n_L(1-n_R)+\mathbb{B}_2n_R(1-n_L)\\+\mathbb{F}n_Ln_R(1-n_L)(1-nR)+\mathbb{J}n_Ln_R(n_L-n_R),\end{aligned} \tag{A3}$$

where

$$\mathbb{C}_1=4e^{-i(\lambda_L+\lambda_R)}\Gamma_L\Gamma_R\big(4\Gamma_L\Gamma_Re^{i(\lambda_L-\lambda_R)}(e^{i\lambda_L}-e^{i\lambda_R})^2\big(\big[F^R_{0,dd}\big]^2-G^R_{0,d\bar{d}}G^R_{0,\bar{d}d}\big)^2-(1-e^{i(\lambda_L+\lambda_R)})^2\big[F^R_{0,dd}\big]^2\big), \tag{A4}$$

$$\mathbb{C}_2=4e^{-i(\lambda_L+\lambda_R)}\Gamma_L\Gamma_R\big(4\Gamma_L\Gamma_Re^{-i(\lambda_L-\lambda_R)}(e^{i\lambda_L}-e^{i\lambda_R})^2\big(\big[F^R_{0,dd}\big]^2-G^R_{0,d\bar{d}}G^R_{0,\bar{d}d}\big)^2-(1-e^{i(\lambda_L+\lambda_R)})^2\big[F^R_{0,dd}\big]^2\big), \tag{A5}$$

$$\begin{aligned}\mathbb{B}_1=4e^{-2i\lambda_L}\big(-2e^{i\lambda_L}(e^{i\lambda_L}-e^{i\lambda_R})\big(\big[F^R_{0,dd}\big]^2-G^R_{0,d\bar{d}}G^R_{0,\bar{d}d}\big)^2\Gamma_L^3\Gamma_R+e^{2i\lambda_L}(-1+e^{2i\lambda_R})\big[F^R_{0,dd}\big]^2\Gamma_R^2\\-e^{i\lambda_L}(e^{i\lambda_L}-e^{i\lambda_R})\Gamma_L\Gamma_R\big(\big[G^R_{0,d\bar{d}}\big]^2+\big[G^R_{0,\bar{d}d}\big]^2+2\big(\big[F^R_{0,dd}\big]^2-G^R_{0,d\bar{d}}G^R_{0,\bar{d}d}\big)^2\Gamma_R^2\big)\\+\Gamma_L^2\big(-(-1+e^{2i\lambda_L})\big[F^R_{0,dd}\big]^2+4e^{i\lambda_R}(-e^{i\lambda_L}+e^{i\lambda_R})\big(\big[F^R_{0,dd}\big]^2-G^R_{0,d\bar{d}}G^R_{0,\bar{d}d}\big)^2\Gamma_R^2\big)\big),\end{aligned} \tag{A6}$$

$$\begin{aligned}\mathbb{B}_2=4e^{-2i\lambda_L}\big(-2e^{i\lambda_L}(e^{i\lambda_L}-e^{i\lambda_R})\big(\big[F^R_{0,dd}\big]^2-G^R_{0,d\bar{d}}G^R_{0,\bar{d}d}\big)^2\Gamma_L^3\Gamma_R\\+e^{2i\lambda_L}(-1+e^{2i\lambda_R})\big[F^R_{0,dd}\big]^2\Gamma_R^2-e^{i\lambda_L}(e^{i\lambda_L}-e^{i\lambda_R})\Gamma_L\Gamma_R\big(\big[G^R_{0,d\bar{d}}\big]^2+\big[G^R_{0,\bar{d}d}\big]^2+2\big(\big[F^R_{0,dd}\big]^2G^R_{0,d\bar{d}}G^R_{0,\bar{d}d}\big)^2\Gamma_R^2\big)\\+\Gamma_L^2\big(-(-1+e^{2i\lambda_L})\big[F^R_{0,dd}\big]^2+4e^{i\lambda_R}(-e^{i\lambda_L}+e^{i\lambda_R})\big(\big[F^R_{0,dd}\big]^2-G^R_{0,d\bar{d}}G^R_{0,\bar{d}d}\big)^2\Gamma_R^2\big)\big),\end{aligned} \tag{A7}$$

$$\mathbb{F}=256\Gamma_L^2\Gamma_R^2\big(\big[F^R_{0,dd}\big]^2-G^R_{0,d\bar{d}}G^R_{0,\bar{d}d}\big)^2\left(\sin\frac{\lambda_L-\lambda_R}{2}\right)^4, \tag{A8}$$

$$\mathbb{J}=128i\Gamma_L^2\Gamma_R^2\big(\big[F^R_{0,dd}\big]^2-G^R_{0,d\bar{d}}G^R_{0,\bar{d}d}\big)^2\left(\sin\frac{\lambda_L-\lambda_R}{2}\right)^2\sin(\lambda_L-\lambda_R), \tag{A9}$$

where the Green functions, i.e., $G_{0,\bar{d}d}$,$G_{0,d\bar{d}}$, and $F_{0,dd}$, are defined in Eqs. (23), (24), and (25) of the main text.

APPENDIX B: CALCULATION OF THE CGF CORRECTIONS DUE TO WEAK INTERACTION EFFECTS

1. Derivation of the interaction correction formula

For the convenience of the calculation, we consider the polarization function (see Fig. 4) in the Schwinger-Keldysh space (without Larkin-Ovchinnikov rotation),

$$\begin{aligned}\hat{\Pi}_{\mathrm{P}}(\Omega) &= \begin{pmatrix} \hat{\Pi}^{T}_{\mathrm{P}}(\Omega) & \hat{\Pi}^{<}_{\mathrm{P}}(\Omega) \\ \hat{\Pi}^{>}_{\mathrm{P}}(\Omega) & \hat{\Pi}^{\widetilde{T}}_{\mathrm{P}}(\Omega) \end{pmatrix} \\ &= i\int_{-\infty}^{\infty}\frac{d\omega_1}{2\pi}\begin{pmatrix} G^{T}_{d\bar{d}}(\omega_1+\Omega)G^{T}_{d\bar{d}}(\omega_1)+F^{T}_{dd}(\omega_1+\Omega)F^{T}_{\bar{d}\bar{d}}(\omega_1) & G^{<}_{d\bar{d}}(\omega_1+\Omega)G^{>}_{d\bar{d}}(\omega_1)+F^{<}_{dd}(\omega_1+\Omega)F^{>}_{\bar{d}\bar{d}}(\omega_1) \\ G^{>}_{d\bar{d}}(\omega_1+\Omega)G^{<}_{d\bar{d}}(\omega_1)+F^{>}_{dd}(\omega_1+\Omega)F^{<}_{\bar{d}\bar{d}}(\omega_1) & G^{\widetilde{T}}_{d\bar{d}}(\omega_1+\Omega)G^{\widetilde{T}}_{d\bar{d}}(\omega_1)+F^{\widetilde{T}}_{dd}(\omega_1+\Omega)F^{\widetilde{T}}_{\bar{d}\bar{d}}(\omega_1) \end{pmatrix}.\end{aligned} \tag{B1}$$

Here the subscript P indicates the particle channel, its particle-hole conjugation (i.e., the hole channel) $\hat{\Pi}_{\mathrm{H}}(\Omega)$ has the same form but with replacement $G_{d\bar{d}} \to G_{\bar{d}d}$ and $F_{dd} \to F_{\bar{d}\bar{d}}$. The respective self-energy for the spin-up channel can be extracted from

$$\Sigma^{\lambda_L}_{d\bar{d},\uparrow}(\omega) = iU^2\int\frac{d\Omega}{2\pi}\begin{pmatrix} G^{T}_{d\bar{d},\uparrow}(\omega-\Omega)\hat{\Pi}^{T}_{\mathrm{P},\downarrow}(\Omega) & G^{<}_{d\bar{d},\uparrow}(\omega-\Omega)\hat{\Pi}^{>}_{\mathrm{P},\downarrow}(\Omega) \\ G^{>}_{d\bar{d},\uparrow}(\omega-\Omega)\hat{\Pi}^{<}_{\mathrm{P},\downarrow}(\Omega) & G^{\widetilde{T}}_{d\bar{d},\uparrow}(\omega-\Omega)\hat{\Pi}^{\widetilde{T}}_{\mathrm{P},\downarrow}(\Omega) \end{pmatrix}, \tag{B2}$$

$$\Sigma^{\lambda_L}_{\bar{d}d,\uparrow}(\omega) = iU^2\int\frac{d\Omega}{2\pi}\begin{pmatrix} F^{T}_{\bar{d}d,\uparrow}(\omega-\Omega)\hat{\Pi}^{T}_{\mathrm{P},\downarrow}(\Omega) & F^{<}_{\bar{d}\bar{d},\uparrow}(\omega-\Omega)\hat{\Pi}^{>}_{\mathrm{P},\downarrow}(\Omega) \\ F^{>}_{\bar{d}\bar{d},\uparrow}(\omega-\Omega)\hat{\Pi}^{<}_{\mathrm{P},\downarrow}(\Omega) & F^{\widetilde{T}}_{\bar{d}\bar{d},\uparrow}(\omega-\Omega)\Pi^{\hat{}}_{,\downarrow}{}^{\widetilde{T}}_{\mathrm{P}}(\Omega) \end{pmatrix}, \tag{B3}$$

$$\Sigma^{\lambda_L}_{dd,\uparrow}(\omega) = iU^2\int\frac{d\Omega}{2\pi}\begin{pmatrix} F^{T}_{dd,\uparrow}(\omega-\Omega)\hat{\Pi}^{T}_{\mathrm{H},\downarrow}(\Omega) & F^{<}_{dd,\uparrow}(\omega-\Omega)\hat{\Pi}^{>}_{\mathrm{H},\downarrow}(\Omega) \\ F^{>}_{dd,\uparrow}(\omega-\Omega)\hat{\Pi}^{<}_{\mathrm{H},\downarrow}(\Omega) & F^{\widetilde{T}}_{dd,\uparrow}(\omega-\Omega)\hat{\Pi}^{\widetilde{T}}_{\mathrm{H},\downarrow}(\Omega) \end{pmatrix}, \tag{B4}$$

$$\Sigma^{\lambda_L}_{\bar{d}\bar{d},\uparrow}(\omega) = iU^2\int\frac{d\Omega}{2\pi}\begin{pmatrix} G^{T}_{\bar{d}d,\uparrow}(\omega-\Omega)\hat{\Pi}^{T}_{\mathrm{H},\downarrow}(\Omega) & G^{<}_{\bar{d}d,\uparrow}(\omega-\Omega)\hat{\Pi}^{>}_{\mathrm{H},\downarrow}(\Omega) \\ G^{>}_{\bar{d}d,\uparrow}(\omega-\Omega)\hat{\Pi}^{<}_{\mathrm{H},\downarrow}(\Omega) & G^{\widetilde{T}}_{\bar{d}d,\uparrow}(\omega-\Omega)\hat{\Pi}^{\widetilde{T}}_{\mathrm{H},\downarrow}(\Omega) \end{pmatrix}, \tag{B5}$$

where the spin-up channel couples to MZM and the spin-down channel does not. We want to calculate the following function, i.e., interaction correction in Eq. (55),

$$\begin{aligned}&\int_{-\infty}^{\infty}\frac{d\omega}{2\pi}\mathrm{Tr}\big(\breve{\mathrm{Q}}^{\lambda_{\mathrm{L}}}_{\mathrm{dd},\uparrow,\mathrm{U}=0}(\omega)\Sigma^{\lambda_{\mathrm{L}}}_{\uparrow}(\omega)\big) \\ &= \int_{-\infty}^{\infty}\frac{d\omega}{2\pi}\mathrm{Tr}\big(\mathrm{G}_{\mathrm{d\bar{d}},\uparrow}(\omega)\Sigma^{\lambda_{\mathrm{L}}}_{\mathrm{d\bar{d}},\uparrow}(\omega)+\mathrm{F}_{\mathrm{dd},\uparrow}(\omega)\Sigma^{\lambda_{\mathrm{L}}}_{\mathrm{\bar{d}\bar{d}},\uparrow}(\omega)+\mathrm{F}_{\mathrm{\bar{d}\bar{d}},\uparrow}(\omega)\Sigma^{\lambda_{\mathrm{L}}}_{\mathrm{dd},\uparrow}(\omega)+\mathrm{G}_{\mathrm{\bar{d}d},\uparrow}(\omega)\Sigma^{\lambda_{\mathrm{L}}}_{\mathrm{\bar{d}d},\uparrow}(\omega)\big) \\ &= \int_{-\infty}^{\infty}\frac{d\omega}{2\pi}\mathrm{Tr}\big(\gamma^{\mathrm{cl}}\mathrm{G}_{\mathrm{d\bar{d}},\uparrow}(\omega)\gamma^{\mathrm{cl}}\Sigma^{\lambda_{\mathrm{L}}}_{\mathrm{d\bar{d}},\uparrow}(\omega)+\gamma^{\mathrm{cl}}\mathrm{F}_{\mathrm{dd},\uparrow}(\omega)\gamma^{\mathrm{cl}}\Sigma^{\lambda_{\mathrm{L}}}_{\mathrm{\bar{d}\bar{d}},\uparrow}(\omega)+\gamma^{\mathrm{cl}}\mathrm{F}_{\mathrm{\bar{d}\bar{d}},\uparrow}(\omega)\gamma^{\mathrm{cl}}\Sigma^{\lambda_{\mathrm{L}}}_{\mathrm{dd},\uparrow}(\omega)+\gamma^{\mathrm{cl}}\mathrm{G}_{\mathrm{\bar{d}d},\uparrow}(\omega)\gamma^{\mathrm{cl}}\Sigma^{\lambda_{\mathrm{L}}}_{\mathrm{\bar{d}d},\uparrow}(\omega)\big),\end{aligned} \tag{B6}$$

where $\gamma^{cl} = \mathbb{I}_{2\times 2}$. Note that the matrix Green functions and self-energies [which are from Eq.(55)] have the form $\left(\begin{smallmatrix} G^{R} & G^{K} \\ G^{\breve{K}} & G^{A} \end{smallmatrix}\right)$ (i.e., with the L-O rotation). Therefore, the function above just corresponds to the classical-classical part ($\widetilde{K}$) of a certain polarization function, and we define a function $\Xi^{\widetilde{K}}_{\lambda,\sigma}$ for the interaction correction,

$$U^2\,\Xi^{\widetilde{K}}_{\lambda,\uparrow} = \int_{-\infty}^{\infty}\frac{d\omega}{2\pi}\mathrm{Tr}\big(\gamma^{\mathrm{cl}}\mathrm{G}_{\mathrm{d\bar{d}},\uparrow}(\omega)\gamma^{\mathrm{cl}}\Sigma^{\lambda_{\mathrm{L}}}_{\mathrm{d\bar{d}},\uparrow}(\omega)+\gamma^{\mathrm{cl}}\mathrm{F}_{\mathrm{dd},\uparrow}(\omega)\gamma^{\mathrm{cl}}\Sigma^{\lambda_{\mathrm{L}}}_{\mathrm{\bar{d}\bar{d}},\uparrow}(\omega)+\gamma^{\mathrm{cl}}\mathrm{F}_{\mathrm{\bar{d}\bar{d}},\uparrow}(\omega)\gamma^{\mathrm{cl}}\Sigma^{\lambda_{\mathrm{L}}}_{\mathrm{dd},\uparrow}(\omega)+\gamma^{\mathrm{cl}}\mathrm{G}_{\mathrm{\bar{d}d},\uparrow}(\omega)\gamma^{\mathrm{cl}}\Sigma^{\lambda_{\mathrm{L}}}_{\mathrm{\bar{d}d},\uparrow}(\omega)\big), \tag{B7}$$

which can be described by the diagrams shown in Fig. 5. The function Ξ_λ in the Schwinger-Keldysh space (without L-O rotation) has the simple form,

$$\Xi_\lambda = \begin{pmatrix} \Xi^{T}_{\lambda} & \Xi^{<}_{\lambda} \\ \Xi^{>}_{\lambda} & \Xi^{\widetilde{T}}_{\lambda} \end{pmatrix}, \tag{B8}$$

where

$$\Xi^{T}_{\lambda} = \int_{-\infty}^{\infty}\frac{d\Omega}{2\pi}\big(\hat{\Pi}^{T}_{P,\uparrow}(-\Omega)\hat{\Pi}^{T}_{P,\downarrow}(\Omega)+\hat{\Pi}^{T}_{H,\uparrow}(-\Omega)\hat{\Pi}^{T}_{H,\downarrow}(\Omega)\big), \tag{B9}$$

$$\Xi^{\widetilde{T}}_{\lambda} = \int_{-\infty}^{\infty}\frac{d\Omega}{2\pi}\big(\hat{\Pi}^{\widetilde{T}}_{P,\uparrow}(-\Omega)\hat{\Pi}^{\widetilde{T}}_{P,\downarrow}(\Omega)+\hat{\Pi}^{\widetilde{T}}_{H,\uparrow}(-\Omega)\hat{\Pi}^{\widetilde{T}}_{H,\downarrow}(\Omega)\big), \tag{B10}$$

$$\Xi_\lambda^< = \int_{-\infty}^{\infty} \frac{d\Omega}{2\pi} (\hat{\Pi}^<_{P,\uparrow}(-\Omega)\hat{\Pi}^<_{P,\downarrow}(\Omega) + \hat{\Pi}^<_{H,\uparrow}(-\Omega)\hat{\Pi}^<_{H,\downarrow}(\Omega)), \tag{B11}$$

$$\Xi_\lambda^> = \int_{-\infty}^{\infty} \frac{d\Omega}{2\pi} (\hat{\Pi}^>_{P,\uparrow}(-\Omega)\hat{\Pi}^>_{P,\downarrow}(\Omega) + \hat{\Pi}^>_{H,\uparrow}(-\Omega)\hat{\Pi}^>_{H,\downarrow}(\Omega)), \tag{B12}$$

and

$$\Xi_\lambda^{\widetilde{K}} = \left(\Xi_\lambda^T + \Xi_\lambda^{\widetilde{T}} - \Xi_\lambda^< - \Xi_\lambda^>\right)/2. \tag{B13}$$

Finally, we reach the formula in Eq. (56) of the main text.

2. Expansion of $\Xi_\lambda^{\widetilde{K}}$

Now, let's look at how the correction $\Xi_\lambda^{\widetilde{K}}$ changes as a function of source-drain bias eV for $T = 0$. For small eV, we can expand the function,

$$\Xi_\lambda^{\widetilde{K}}(eV) = \Xi_\lambda^{\widetilde{K}}(0) + (eV)\Xi_\lambda^{\widetilde{K},(1)}(0) + (eV)^2\Xi_\lambda^{\widetilde{K},(2)}(0) + (eV)^3\Xi_\lambda^{\widetilde{K},(3)}(0) + \cdots. \tag{B14}$$

Due to the causality reasons (this is still true in the presence of the artificial counting field), the polarization function at $T = 0$ and $eV = 0$ has the following properties: $\hat{\Pi}^<_{P,\sigma}(\Omega) \propto n(\Omega)$ and $\hat{\Pi}^>_{P,\sigma}(\Omega) \propto 1 - n(\Omega)$, where $n(\Omega) = 1 - \theta(\Omega)$ is the Fermi-distribution function at $T = 0$. Then, we find $\Xi_\lambda^<(eV = 0) = 0$ and $\Xi_\lambda^>(eV = 0) = 0$ for $T = 0$. Although the time-ordered and anti-time-ordered parts of the Green functions ($G^{T,\widetilde{T}}_{d\bar{d}}, G^{T,\widetilde{T}}_{\bar{d}d}, F^{T,\widetilde{T}}_{dd}$, and $F^{T,\widetilde{T}}_{\bar{d}\bar{d}}$) depend on the counting field λ_L, their dependence on λ_L enters in such a way that all the λ_L-dependent terms have a prefactor $n_L(1 - n_R)$. At $T = 0$ and $eV = 0$, $n_L(1 - n_R)$ vanishes and time-order and anti-time-order Green functions are independent of λ_L. Therefore, we have $\Xi_\lambda^T(eV = 0) = \Xi_{\lambda=0}^T(eV = 0)$ and $\Xi_\lambda^{\widetilde{T}}(eV = 0) = \Xi_{\lambda=0}^{\widetilde{T}}(eV = 0)$. Combining those relations with $\Xi_{\lambda=0}^{\widetilde{K}}(eV = 0) = \Xi_{\lambda=0}^T(eV = 0) + \Xi_{\lambda=0}^{\widetilde{T}}(eV = 0) = 0$, we can show

$$\Xi_\lambda^{\widetilde{K}}(0) = 0. \tag{B15}$$

This is intuitively obvious since there should be no current in equilibrium (i.e., $eV \to 0$).

To consider higher order terms, we expand the integrand of the polarization function integral in order of eV. These integrands have the following form,

$$F^\alpha(\omega_1,\Omega|n_L(\omega_1+\Omega),n_L(\omega_1),n_R(\omega_1+\Omega),n_R(\omega_1)) = G^\alpha_{d\bar{d}}(\omega_1+\Omega)G^\alpha_{d\bar{d}}(\omega_1) + F^\alpha_{dd}(\omega_1+\Omega)F^\alpha_{\bar{d}\bar{d}}(\omega_1), \tag{B16}$$

where $\alpha = T, \widetilde{T}, \langle, \rangle$, The bias eV only enters through the Fermi distribution function n_L and n_R: $n_L(\omega) = 1 - \theta(\omega - eV/2)$, $n_R(\omega) = 1 - \theta(\omega + eV/2)$. Due to the properties of Heaviside theta function, by expansion and resummation, one can prove the following relation: If one has a series of functions $n_i(\omega) = 1 - \theta(\omega - \omega_i)$ with $i = 1,2,\ldots,k$ and $\omega_1 \leqslant \omega_2 \leqslant \cdots \leqslant \omega_k$, then

$$\begin{aligned} F(n_1,n_2,\ldots,n_k) = {} & F(0,0,\ldots,0) + [F(1,1,\ldots,1) - F(0,1,\ldots,1)]n_1 \\ & + \cdots + [F(\overbrace{0,\ldots,0}^{i},1,\ldots,1) - F(\overbrace{0,\ldots,0}^{i+1},1,\ldots,1)]n_i \\ & + \cdots + [F(0,\ldots,0,1) - F(0,0,\ldots,0)]n_k. \end{aligned} \tag{B17}$$

Note that this formula depends on the order of the arguments in the Fermi distribution function. We then define the polarization function for different regions where the function F has different forms. First of all, we consider $\Omega \geqslant eV$ such that $-eV/2 - \Omega < eV/2 - \Omega \leqslant -eV/2 < eV/2$, and define

$$\hat{\Pi}^\alpha_{P1,\sigma}(\Omega,eV) = i\int_{-\infty}^{\infty} \frac{d\omega_1}{2\pi} F_1^\alpha(\omega_1,\Omega), \tag{B18}$$

and $F_1^\alpha(\omega_1,\Omega|n_R(\omega_1+\Omega),n_L(\omega_1+\Omega),n_R(\omega_1),n_L(\omega_1)) = F^\alpha(\omega_1,\Omega|n_L(\omega_1+\Omega),n_L(\omega_1),n_R(\omega_1+\Omega),n_R(\omega_1))$, where F^α is the same function as the one defined in Eq. (B16), but the arguments in the function F_1^α have the different order. Second, we consider $0 < \Omega < eV$ such that $-eV/2 - \Omega < -eV/2 < eV/2 - \Omega < eV/2$, and define

$$\hat{\Pi}^\alpha_{P2,\sigma}(\Omega,eV) = i\int_{-\infty}^{\infty} \frac{d\omega_1}{2\pi} F_2^\alpha(\omega_1,\Omega), \tag{B19}$$

where $F_2^\alpha(\omega_1,\Omega|n_R(\omega_1+\Omega),n_R(\omega_1),n_L(\omega_1+\Omega),n_L(\omega_1)) = F^\alpha(\omega_1,\Omega|n_L(\omega_1+\Omega),n_L(\omega_1),n_R(\omega_1+\Omega),n_R(\omega_1))$. Third, we consider $-eV < \Omega < 0$ such that $-eV/2 < -eV/2 - \Omega < eV/2 < eV/2 - \Omega$, and define

$$\hat{\Pi}^\alpha_{P3,\sigma}(\Omega,eV) = i\int_{-\infty}^{\infty} \frac{d\omega_1}{2\pi} F_3^\alpha(\omega_1,\Omega), \tag{B20}$$

where $F_3^\alpha(\omega_1,\Omega|n_R(\omega_1),n_R(\omega_1+\Omega),n_L(\omega_1),n_L(\omega_1+\Omega)) = F^\alpha(\omega_1,\Omega|n_L(\omega_1+\Omega),n_L(\omega_1),n_R(\omega_1+\Omega),n_R(\omega_1))$. Finally, we consider $\Omega < -eV$ such that $-eV/2 < eV/2 < -eV/2-\Omega < eV/2-\Omega$, and define

$$\hat{\Pi}^\alpha_{P4,\sigma}(\Omega,eV) = i\int_{-\infty}^{\infty}\frac{d\omega_1}{2\pi}F_4^\alpha(\omega_1,\Omega), \tag{B21}$$

where $F_4^\alpha(\omega_1,\Omega|n_R(\omega_1),n_L(\omega_1),n_R(\omega_1+\Omega),n_L(\omega_1+\Omega)) = F^\alpha(\omega_1,\Omega|n_L(\omega_1+\Omega),n_L(\omega_1),n_R(\omega_1+\Omega),n_R(\omega_1))$.

Following the definition above, the correction $\Xi_\lambda^{\widetilde{K}}$ can be written as (here we consider $\epsilon_d = 0$)

$$\Xi^\alpha_\lambda = \Xi^\alpha_{\lambda,A} + \Xi^\alpha_{\lambda,B}, \tag{B22}$$

where

$$\begin{aligned}
\Xi^\alpha_{\lambda,A} &= 2\int_0^\infty\frac{d\Omega}{2\pi}\hat{\Pi}^\alpha_{P1,\uparrow}(\Omega)\hat{\Pi}_{P4,\downarrow}(-\Omega)^\alpha + 2\int_{-\infty}^0\frac{d\Omega}{2\pi}\hat{\Pi}^\alpha_{P4,\uparrow}(\Omega)\hat{\Pi}^\alpha_{P1,\downarrow}(-\Omega),\\
\Xi^\alpha_{\lambda,B} &= 2\int_0^{eV}\frac{d\Omega}{2\pi}\big[\hat{\Pi}^\alpha_{P2,\uparrow}(\Omega)\hat{\Pi}_{P3,\downarrow}(-\Omega)^\alpha - \hat{\Pi}^\alpha_{P1,\uparrow}(\Omega)\hat{\Pi}_{P4,\downarrow}(-\Omega)^\alpha\big]\\
&\quad + 2\int_{-eV}^0\frac{d\Omega}{2\pi}\big[\hat{\Pi}^\alpha_{P3,\uparrow}(\Omega)\hat{\Pi}_{P2,\downarrow}(-\Omega)^\alpha - \hat{\Pi}^\alpha_{P4,\uparrow}(\Omega)\hat{\Pi}_{P1,\downarrow}(-\Omega)^\alpha\big]\\
&= \Xi^\alpha_{\lambda,A} + \Xi^\alpha_{\lambda,B}.
\end{aligned} \tag{B23}$$

Here the factor 2 comes from the summation of both particle and hole parts (note that $\hat{\Pi}_{P,\sigma} = \hat{\Pi}_{H,\sigma}$ for $\epsilon_d = 0$). The whole correction includes two parts: the first part $\Xi^\alpha_{\lambda,A}$ and a leftover part $\Xi^\alpha_{\lambda,B}$. To check this formalism, we considered the case without MZM coupling and reproduce the result shown in Eq. (21) of Gogolin and Komnik [68]. Note, in order to obtain the right result, we need to take the appropriate order of limits. If we want to reproduce the $\kappa = 0$ result, we have to take the limit $\kappa \to 0$ before taking the $\omega \to 0$ limit for linear response. Then, we focus on the case with MZM coupling (where if we want to consider zero Majorana splitting, i.e., $\delta = 0$, we have to take the limit $\delta \to 0$ first before taking the $\omega \to 0$ limit for linear response).

3. Derivation of the first part of interaction correction $\Xi^{\widetilde{K},(2)}_{\lambda,A}$

First of all, we focus on the first part $\Xi^\alpha_{\lambda,A}$, and expand it in order of eV. We also notice that after the transformation of Eq. (B17), the integrands of the polarization functions are linear in the Fermi distribution function. Therefore, the expansion can be obtained analytically by expanding the Fermi distribution function,

$$n\left(\omega \pm \frac{eV}{2}\right) = n(\omega) - \delta(\omega)\left(\pm\frac{eV}{2}\right) - \frac{1}{2!}\delta'(\omega)\left(\pm\frac{eV}{2}\right)^2 - \frac{1}{3!}\delta''(\omega)\left(\pm\frac{eV}{2}\right)^3 + \cdots. \tag{B24}$$

After expanding the Fermi distribution function in order of eV, we further expand the polarization function,

$$\hat{\Pi}_P(\Omega,eV) = \hat{\Pi}_P(\Omega,0) + (eV)\hat{\Pi}^{(1)}_P(\Omega,0) + (eV)^2\hat{\Pi}^{(2)}_P(\Omega,0) + (eV)^3\hat{\Pi}^{(3)}_P(\Omega,0) + \cdots. \tag{B25}$$

After the integration by part for the Dirac-delta function, the linear terms can be obtained:

$$\begin{aligned}
\hat{\Pi}^{\alpha,(1)}_P(\Omega>0,0) = \frac{i}{4\pi}\big[&-F_1^\alpha(-\Omega,\Omega|1,1,1,1) + 2F_1^\alpha(-\Omega,\Omega|0,1,1,1) - F_1^\alpha(-\Omega,\Omega|0,0,1,1)\\
&- F_1^\alpha(0,\Omega|0,0,1,1) + 2F_1^\alpha(0,\Omega|0,0,0,1) - F_1^\alpha(0,\Omega|0,0,0,0)\big],
\end{aligned} \tag{B26}$$

$$\begin{aligned}
\hat{\Pi}^{\alpha,(1)}_P(\Omega<0,0) = \frac{i}{4\pi}\big[&-F_4^\alpha(0,\Omega|1,1,1,1) + 2F_4^\alpha(0,\Omega|0,1,1,1) - F_4^\alpha(0,\Omega|0,0,1,1)\\
&- F_4^\alpha(-\Omega,\Omega|0,0,1,1) + 2F_4^\alpha(-\Omega,\Omega|0,0,0,1) - F_4^\alpha(-\Omega,\Omega|0,0,0,0)\big],
\end{aligned} \tag{B27}$$

where $\alpha = T,\widetilde{T},\langle,\rangle$. After simplification of those expressions above, we find for both spin channels at $T = 0$,

$$\hat{\Pi}^{T,(1)}_P(\Omega,0) = 0, \quad \hat{\Pi}^{\widetilde{T},(1)}_P(\Omega,0) = 0, \quad \hat{\Pi}^{<,(1)}_P(\Omega,0) \sim \theta(-\Omega), \quad \hat{\Pi}^{>,(1)}_P(\Omega,0) \sim \theta(\Omega). \tag{B28}$$

We then obtain the linear correction to the generating function,

$$\begin{aligned}
\Xi^{\widetilde{K},(1)}_\lambda(0) = 2\int_{-\infty}^\infty\frac{d\Omega}{2\pi}\big[&\hat{\Pi}^T_{P,\uparrow}(-\Omega,0)\hat{\Pi}^{T,(1)}_{P,\downarrow}(\Omega,0) + \hat{\Pi}^{\widetilde{T}}_{P,\uparrow}(-\Omega,0)\hat{\Pi}^{\widetilde{T},(1)}_{P,\downarrow}(\Omega,0) + \hat{\Pi}^<_{P,\uparrow}(-\Omega,0)\hat{\Pi}^{<,(1)}_{P,\downarrow}(\Omega,0)\\
&+ \hat{\Pi}^>_{P,\uparrow}(-\Omega,0)\hat{\Pi}^{>,(1)}_{P,\downarrow}(\Omega,0) + \hat{\Pi}^{T,(1)}_{P,\uparrow}(-\Omega,0)\hat{\Pi}^T_{P,\downarrow}(\Omega,0) + \hat{\Pi}^{\widetilde{T},(1)}_{P,\uparrow}(-\Omega,0)\hat{\Pi}^{\widetilde{T}}_{P,\downarrow}(\Omega,0)\\
&+ \hat{\Pi}^{<,(1)}_{P,\uparrow}(-\Omega,0)\hat{\Pi}^<_{P,\downarrow}(\Omega,0) + \hat{\Pi}^{>,(1)}_{P,\uparrow}(-\Omega,0)\hat{\Pi}^>_{P,\downarrow}(\Omega,0)\big]\\
= 0.&
\end{aligned} \tag{B29}$$

Similarly, the quadratic terms can be written as

$$\hat{\Pi}_P^{\alpha,(2)}(\Omega>0,0)=\frac{i}{16\pi}\big[\partial_{\omega_1}F_1^{\alpha}(\omega_1=-\Omega,\Omega|1,1,1,1)-\partial_{\omega_1}F_1^{\alpha}(\omega_1=-\Omega,\Omega|0,0,1,1)+\partial_{\omega_1}F_1^{\alpha}(\omega_1=0,\Omega|0,0,1,1)-\partial_{\omega_1}F_1^{\alpha}(\omega_1=0,\Omega|0,0,0,0)\big], \tag{B30}$$

$$\hat{\Pi}_P^{\alpha,(2)}(\Omega<0,0)=\frac{i}{16\pi}\big[\partial_{\omega_1}F_4^{\alpha}(\omega_1=-\Omega,\Omega|1,1,1,1)-\partial_{\omega_1}F_4^{\alpha}(\omega_1=-\Omega,\Omega|0,0,1,1)+\partial_{\omega_1}F_4^{\alpha}(\omega_1=0,\Omega|0,0,1,1)-\partial_{\omega_1}F_4^{\alpha}(\omega_1=0,\Omega|0,0,0,0)\big]. \tag{B31}$$

The quadratic term of the generating function is, therefore,

$$\Xi_{\lambda}^{\widetilde{K},(2)}(0)=2\int_{-\infty}^{\infty}\frac{d\Omega}{2\pi}\big[\hat{\Pi}_{P,\uparrow}^{T}(-\Omega,0)\hat{\Pi}_{P,\downarrow}^{T,(2)}(\Omega,0)+\hat{\Pi}_{P,\uparrow}^{\widetilde{T}}(-\Omega,0)\hat{\Pi}_{P,\downarrow}^{\widetilde{T},(2)}(\Omega,0)+\hat{\Pi}_{P,\uparrow}^{T,(2)}(-\Omega,0)\hat{\Pi}_{P,\downarrow}^{T}(\Omega,0)+\hat{\Pi}_{P,\uparrow}^{\widetilde{T},(2)}(-\Omega,0)\hat{\Pi}_{P,\downarrow}^{\widetilde{T}}(\Omega,0)\big], \tag{B32}$$

where we use the relations $\hat{\Pi}^{>}(-\Omega,0)\hat{\Pi}^{>}(\Omega,0)=0$, $\hat{\Pi}^{<}(-\Omega,0)\hat{\Pi}^{<}(\Omega,0)=0$, $\hat{\Pi}^{(1),T}(-\Omega,0)=0$, and $\hat{\Pi}^{(1),\widetilde{T}}(-\Omega,0)=0$. After the simplification of polarization functions, we find that the time-ordered and anti-time-ordered parts $\hat{\Pi}_P^{\alpha,(2)}(\Omega,0)$ (for $\alpha=T,\widetilde{T}$) do not depend on the counting field λ_L. Then, we conclude that the quadratic term $\Xi_{\lambda}^{\widetilde{K},(2)}(0)$ is the same as the term with $\lambda_L=0$, which is zero due to causality and unitarity,

$$\Xi_{\lambda}^{\widetilde{K},(2)}(0)=0. \tag{B33}$$

The cubic term of the polarization function corresponds to the integral of δ'', and thus reads

$$\hat{\Pi}_P^{\alpha,(3)}(\Omega>0,0)=\frac{i}{3!2^3 2\pi}\big[-\partial_{\omega_1}^2F_1^{\alpha}(-\Omega,\Omega|1,1,1,1)+2\partial_{\omega_1}^2F_1^{\alpha}(-\Omega,\Omega|0,1,1,1)-\partial_{\omega_1}^2F_1^{\alpha}(-\Omega,\Omega|0,0,1,1)-\partial_{\omega_1}^2F_1^{\alpha}(0,\Omega|0,0,1,1)+2\partial_{\omega_1}^2F_1^{\alpha}(0,\Omega|0,0,1,1)-\partial_{\omega_1}^2F_1^{\alpha}(0,\Omega|0,0,0,0)\big], \tag{B34}$$

$$\hat{\Pi}_P^{\alpha,(3)}(\Omega<0,0)=\frac{i}{3!2^3 2\pi}\big[-\partial_{\omega_1}^2F_4^{\alpha}(0,\Omega|1,1,1,1)+2\partial_{\omega_1}^2F_4^{\alpha}(0,\Omega|0,1,1,1)-\partial_{\omega_1}^2F_4^{\alpha}(0,\Omega|0,0,1,1)-\partial_{\omega_1}^2F_4^{\alpha}(-\Omega,\Omega|0,0,1,1)+2\partial_{\omega_1}^2F_4^{\alpha}(-\Omega,\Omega|0,0,1,1)-\partial_{\omega_1}^2F_4^{\alpha}(-\Omega,\Omega|0,0,0,0)\big]. \tag{B35}$$

We evaluate and simplify the function above for $\epsilon_d=0$ and $\Gamma_L=\Gamma_R=\Gamma/2$, and obtain

$$\hat{\Pi}_{P,\uparrow}^{T,(3)}(\Omega,0)=\frac{-i(e^{i\lambda_L}-1)[(e^{i\lambda_L}-1)\Gamma^2-2(e^{i\lambda_L}+3)\kappa^2]}{48\pi(e^{i\lambda_L}+1)^2\Gamma^2\kappa^2}\frac{1}{(|\Omega|+i\Gamma)^2}, \tag{B36}$$

$$\hat{\Pi}_{P,\uparrow}^{\widetilde{T},(3)}(\Omega,0)=\frac{-i(e^{i\lambda_L}-1)[(e^{i\lambda_L}-1)\Gamma^2-2(e^{i\lambda_L}+3)\kappa^2]}{48\pi(e^{i\lambda_L}+1)^2\Gamma^2\kappa^2}\frac{1}{(|\Omega|-i\Gamma)^2}, \tag{B37}$$

$$\hat{\Pi}_{P,\downarrow}^{T,(3)}(\Omega,0)=\frac{-i(e^{-i\lambda_L}-1)}{12\pi\Gamma^2}\frac{1}{(|\Omega|+i\Gamma)^2}, \tag{B38}$$

$$\hat{\Pi}_{P,\downarrow}^{\widetilde{T},(3)}(\Omega,0)=\frac{-i(e^{-i\lambda_L}-1)}{12\pi\Gamma^2}\frac{1}{(|\Omega|-i\Gamma)^2}. \tag{B39}$$

The cubic term of the generating function reads

$$\begin{aligned}\Xi_{\lambda,A}^{\widetilde{K},(3)}(0)&=2\int_{-\infty}^{\infty}\frac{d\Omega}{2\pi}\big[\hat{\Pi}_{P,\uparrow}^{T}(-\Omega,0)\hat{\Pi}_{P,\downarrow}^{T,(3)}(\Omega,0)+\hat{\Pi}_{P,\uparrow}^{\widetilde{T}}(-\Omega,0)\hat{\Pi}_{P,\downarrow}^{\widetilde{T},(3)}(\Omega,0)\\&\quad+\hat{\Pi}_{P,\uparrow}^{T,(3)}(-\Omega,0)\hat{\Pi}_{P,\downarrow}^{T}(\Omega,0)+\hat{\Pi}_{P,\uparrow}^{\widetilde{T},(3)}(-\Omega,0)\hat{\Pi}_{P,\downarrow}^{\widetilde{T}}(\Omega,0)\big]\\&=\frac{-i(e^{-i\lambda_L}-1)}{6\pi\Gamma^2}\int_{-\infty}^{\infty}\frac{d\Omega}{2\pi}\left[\hat{\Pi}_{P,\uparrow}^{T}(-\Omega,0)\frac{1}{(|\Omega|+i\Gamma)^2}+\hat{\Pi}_{P,\uparrow}^{\widetilde{T}}(-\Omega,0)\frac{1}{(|\Omega|-i\Gamma)^2}\right]\\&\quad+\frac{-i(e^{i\lambda_L}-1)[(e^{i\lambda_L}-1)\Gamma^2-2(e^{i\lambda_L}+3)\kappa^2]}{24\pi(e^{i\lambda_L}+1)^2\Gamma^2\kappa^2}\\&\quad\times\int_{-\infty}^{\infty}\frac{d\Omega}{2\pi}\left[\hat{\Pi}_{P,\downarrow}^{T}(-\Omega,0)\frac{1}{(|\Omega|+i\Gamma)^2}+\hat{\Pi}_{P,\downarrow}^{\widetilde{T}}(-\Omega,0)\frac{1}{(|\Omega|-i\Gamma)^2}\right]\\&=\frac{(e^{-i\lambda_L}-1)}{6\pi\Gamma^4}\mathbf{O}(\widetilde{\kappa})+\left(2-\frac{\pi^2}{4}\right)\frac{(e^{i\lambda_L}-1)[(e^{i\lambda_L}-1)-2(e^{i\lambda_L}+3)\widetilde{\kappa}^2]}{12\pi^3(e^{i\lambda_L}+1)^2\Gamma^4\widetilde{\kappa}^2},\end{aligned} \tag{B40}$$

where

$$\mathbf{O}(\widetilde{\kappa}) = \int_{-\infty}^{\infty} \frac{d\widetilde{\Omega}}{2\pi}\left[\hat{\Pi}^{T}_{P,\uparrow}(-\widetilde{\Omega},0)\frac{-i}{(|\widetilde{\Omega}|+i)^2} + \hat{\Pi}^{\widetilde{T}}_{P,\uparrow}(-\widetilde{\Omega},0)\frac{-i}{(|\widetilde{\Omega}|-i)^2}\right], \quad \text{with} \quad \widetilde{\Omega} = \frac{\Omega}{\Gamma}, \quad \widetilde{\kappa} = \frac{\kappa}{\Gamma}. \tag{B41}$$

This correction is nonzero for $\lambda_L \neq 0$.

4. Derivation of the second part of interaction correction $\Xi^{\widetilde{K},(2)}_{\lambda,B}$

Now, let's consider the leftover terms,

$$\begin{aligned}
&2\int_0^{eV}\frac{d\Omega}{2\pi}\left[\hat{\Pi}^{\alpha}_{P2,\uparrow}(\Omega,eV)\hat{\Pi}^{\alpha}_{P3,\downarrow}(-\Omega,eV) - \hat{\Pi}^{\alpha}_{P1,\uparrow}(\Omega,eV)\hat{\Pi}^{\alpha}_{P4,\downarrow}(-\Omega,eV)\right]\\
&\quad + 2\int_{-eV}^{0}\frac{d\Omega}{2\pi}\left[\hat{\Pi}^{\alpha}_{P3,\uparrow}(\Omega,eV)\hat{\Pi}^{\alpha}_{P2,\downarrow}(-\Omega,eV) - \hat{\Pi}^{\alpha}_{P4,\uparrow}(\Omega,eV)\hat{\Pi}^{\alpha}_{P1,\downarrow}(-\Omega,eV)\right]\\
&\quad = 4\int_0^{eV}\frac{d\Omega}{2\pi}\left[\hat{\Pi}^{\alpha}_{P2,\uparrow}(\Omega,eV)\hat{\Pi}^{\alpha}_{P3,\downarrow}(-\Omega,eV) - \hat{\Pi}^{\alpha}_{P1,\uparrow}(\Omega,eV)\hat{\Pi}^{\alpha}_{P4,\downarrow}(-\Omega,eV)\right].
\end{aligned} \tag{B42}$$

We want to expand the following integral in order of eV,

$$\begin{aligned}
\int_0^{eV}\frac{d\Omega}{2\pi}\hat{\Pi}^{\alpha}_{Pi,\uparrow}(\Omega,eV)\hat{\Pi}^{\alpha}_{Pj,\downarrow}(-\Omega,eV) &= \frac{1}{2\pi}(eV)\hat{\Pi}^{\alpha}_{Pi,\uparrow}(0^+,eV)\hat{\Pi}^{\alpha}_{Pj,\downarrow}(0^-,eV)\\
&\quad + \frac{1}{2\pi}(eV)^2\frac{1}{2!}\left(\frac{\partial\hat{\Pi}^{\alpha}_{Pi,\uparrow}(0^+,eV)}{\partial\Omega}\hat{\Pi}^{\alpha}_{Pj,\downarrow}(0^-,eV) - \hat{\Pi}^{\alpha}_{Pi,\uparrow}(0^+,eV)\frac{\partial\hat{\Pi}^{\alpha}_{Pj,\downarrow}(0^-,eV)}{\partial\Omega}\right)\\
&\quad + \frac{1}{2\pi}(eV)^3\frac{1}{3!}\frac{\partial^2\left[\hat{\Pi}^{\alpha}_{Pi,\uparrow}(\Omega,eV)\hat{\Pi}^{\alpha}_{Pj,\downarrow}(-\Omega,eV)\right]}{\partial\Omega^2}\bigg|_{\Omega\to 0^+} + \cdots.
\end{aligned} \tag{B43}$$

In the next step, we will expand the functions $\hat{\Pi}^{\alpha}_{Pi,\sigma}(0^{\pm},eV)\partial_{\Omega}\hat{\Pi}^{\alpha}_{Pi,\sigma}(0^{\pm},eV)$ and $\partial^2_{\Omega}\hat{\Pi}^{\alpha}_{Pi,\sigma}(0^{\pm},eV)$ in the order of eV. The way to expand $\hat{\Pi}^{\alpha}_{Pi,\sigma}(0^{\pm},eV)$ can be found in Appendix B 3. For the $\partial_{\Omega}\hat{\Pi}^{\alpha}_{Pi,\sigma}(0^{\pm},eV)$, for example, we notice that

$$\begin{aligned}
\frac{\partial\hat{\Pi}^{\alpha}_{P2}(\Omega,eV)}{\partial\Omega} &= \frac{i}{2\pi}\frac{\partial}{\partial_{\Omega}}\int_{-\infty}^{\infty}F^{\alpha}_2(\omega_1,\Omega|n_R(\omega_1+\Omega),n_R(\omega_1),n_L(\omega_1+\Omega),n_L(\omega_1))d\omega_1\\
&= \frac{i}{2\pi}\int_{-\infty}^{\infty}\{\partial_{\Omega}F_2(\omega_1,\Omega|0,0,0,0) + [\partial_{\Omega}F_2(\omega_1,\Omega|1,1,1,1) - \partial_{\Omega}F_2(\omega_1,\Omega|0,1,1,1)]n_R(\omega_1+\Omega)\\
&\quad + [\partial_{\Omega}F_2(\omega_1,\Omega|0,1,1,1) - \partial_{\Omega}F_2(\omega_1,\Omega|0,0,1,1)]n_R(\omega_1)\\
&\quad + [\partial_{\Omega}F_2(\omega_1,\Omega|0,0,1,1) - \partial_{\Omega}F_2(\omega_1,\Omega|0,0,0,1)]n_L(\omega_1+\Omega)\\
&\quad + [\partial_{\Omega}F_2(\omega_1,\Omega|0,0,0,1) - \partial_{\Omega}F_2(\omega_1,\Omega|0,0,0,0)]n_L(\omega_1)\}d\omega_1\\
&\quad - \frac{i}{2\pi}\left[F_2\left(-\Omega-\frac{eV}{2},\Omega|1,1,1,1\right) - F_2\left(-\Omega-\frac{eV}{2},\Omega|0,1,1,1\right)\right]\\
&\quad - \frac{i}{2\pi}\left[F_2\left(-\Omega+\frac{eV}{2},\Omega|0,0,1,1\right) - F_2\left(-\Omega+\frac{eV}{2},\Omega|0,0,01,1\right)\right].
\end{aligned} \tag{B44}$$

Similarly, for $\partial_{\Omega}\hat{\Pi}^{\alpha}_{Pj}(\Omega,eV)$ with $j = 1,3,4$. Then, to expand the whole function, we just need to expand the Fermi distribution function and the function F_2 in order of eV, which is very straightforward. For the second derivative $\partial^2_{\Omega}\hat{\Pi}^{\alpha}_{Pi,\sigma}(0^{\pm},eV)$, we can apply the same strategy. Combing all the terms together, we recover Eq. (62).

[1] E. S. Reich, Nature (London) **483**, 132 (2012).
[2] P. W. Brouwer, Science **336**, 989 (2012).
[3] F. Wilczek, Nature (London) **486**, 195 (2012).
[4] J. Alicea, Rep. Prog. Phys. **75**, 076501 (2012).
[5] G. Moore and N. Read, Nucl. Phys. B **360**, 362 (1991).
[6] C. Nayak and F. Wilczek, Nucl. Phys. B **479**, 529 (1996).
[7] N. Read and D. Green, Phys. Rev. B **61**, 10267 (2000).
[8] C. Nayak, S. H. Simon, A. Stern, M. Freedman, and S. Das Sarma, Rev. Mod. Phys. **80**, 1083 (2008).
[9] L. Fu and C. L. Kane, Phys. Rev. Lett. **100**, 096407 (2008).
[10] L. Fu and C. L. Kane, Phys. Rev. B **79**, 161408(R) (2009).
[11] J. D. Sau, R. M. Lutchyn, S. Tewari, and S. Das Sarma, Phys. Rev. Lett. **104**, 040502 (2010).
[12] J. Alicea, Phys. Rev. B **81**, 125318 (2010).

[13] R. M. Lutchyn, J. D. Sau, and S. Das Sarma, Phys. Rev. Lett. **105**, 077001 (2010).
[14] Y. Oreg, G. Refael, and F. von Oppen, Phys. Rev. Lett. **105**, 177002 (2010).
[15] A. Cook and M. Franz, Phys. Rev. B **84**, 201105 (2011).
[16] J. D. Sau and S. D. Sarma, Nat. Commun. **3**, 964 (2012).
[17] S. Nadj-Perge, I. K. Drozdov, B. A. Bernevig, and A. Yazdani, Phys. Rev. B **88**, 020407(R) (2013).
[18] C. W. J. Beenakker, Annu. Rev. Condens. Matter Phys. **4**, 113 (2013).
[19] S. Das Sarma, M. Freedman, and C. Nayak, NPJ Quantum Inf., **1**, 15001 (2015).
[20] A. Y. Kitaev, Phys.-Usp. **44**, 131 (2001).
[21] V. Mourik, K. Zuo, S. M. Frolov, S. R. Plissard, E. P. A. M. Bakkers, and L. P. Kouwenhoven, Science **336**, 1003 (2012).
[22] T. D. Stanescu, R. M. Lutchyn, and S. Das Sarma, Phys. Rev. B **84**, 144522 (2011).
[23] A. Das, Y. Ronen, Y. Most, Y. Oreg, M. Heiblum, and H. Shtrikman, Nat. Phys. **8**, 887 (2012).
[24] M. T. Deng, C. L. Yu, G. Y. Huang, M. Larsson, P. Caroff, and H. Q. Xu, Nano Lett. **12**, 6414 (2012).
[25] A. D. K. Finck, D. J. Van Harlingen, P. K. Mohseni, K. Jung, and X. Li, Phys. Rev. Lett. **110**, 126406 (2013).
[26] H. O. H. Churchill, V. Fatemi, K. Grove-Rasmussen, M. T. Deng, P. Caroff, H. Q. Xu, and C. M. Marcus, Phys. Rev. B **87**, 241401 (2013).
[27] S. Nadj-Perge, I. K. Drozdov, J. Li, H. Chen, S. Jeon, J. Seo, A. H. MacDonald, B. A. Bernevig, and A. Yazdani, Science **346**, 602 (2014).
[28] M. T. Deng, C. L. Yu, G. Y. Huang, M. Larsson, P. Caroff, and H. Q. Xu, Sci. Rep. **4**, 7261 (2014).
[29] E. J. H. Lee, X. Jiang, R. Aguado, G. Katsaros, C. M. Lieber, and S. De Franceschi, Phys. Rev. Lett. **109**, 186802 (2012).
[30] J.-D. Pillet, P. Joyez, R. Žitko, and M. F. Goffman, Phys. Rev. B **88**, 045101 (2013).
[31] J. Liu, A. C. Potter, K. T. Law, and P. A. Lee, Phys. Rev. Lett. **109**, 267002 (2012).
[32] P. Neven, D. Bagrets, and A. Altland, New J. Phys. **15**, 055019 (2013).
[33] A. M. Lobos, R. M. Lutchyn, and S. Das Sarma, Phys. Rev. Lett. **109**, 146403 (2012).
[34] J. D. Sau and S. Das Sarma, Phys. Rev. B **88**, 064506 (2013).
[35] H.-Y. Hui, J. D. Sau, and S. Das Sarma, Phys. Rev. B **90**, 174206 (2014).
[36] D. Bagrets and A. Altland, Phys. Rev. Lett. **109**, 227005 (2012).
[37] D. I. Pikulin, J. P. Dahlhaus, M. Wimmer, H. Schomerus, and C. W. J. Beenakker, New J. Phys. **14**, 125011 (2012).
[38] L. Fidkowski, J. Alicea, N. H. Lindner, R. M. Lutchyn, and M. P. A. Fisher, Phys. Rev. B **85**, 245121 (2012).
[39] R. M. Lutchyn and J. H. Skrabacz, Phys. Rev. B **88**, 024511 (2013).
[40] L. P. Rokhinson, X. Liu, and J. K. Furdyna, Nat. Phys. **8**, 795 (2012).
[41] M. Leijnse and K. Flensberg, Phys. Rev. B **84**, 140501 (2011).
[42] D. E. Liu and H. U. Baranger, Phys. Rev. B **84**, 201308 (2011).
[43] A. Golub, I. Kuzmenko, and Y. Avishai, Phys. Rev. Lett. **107**, 176802 (2011).
[44] M. Lee, J. S. Lim, and R. López, Phys. Rev. B **87**, 241402 (2013).
[45] E. Vernek, P. H. Penteado, A. C. Seridonio, and J. C. Egues, Phys. Rev. B **89**, 165314 (2014).
[46] M. Cheng, M. Becker, B. Bauer, and R. M. Lutchyn, Phys. Rev. X **4**, 031051 (2014).
[47] S. Das Sarma, C. Nayak, and S. Tewari, Phys. Rev. B **73**, 220502 (2006).
[48] E. Grosfeld and A. Stern, Proc. Natl. Acad. Sci. USA **108**, 11810 (2011).
[49] L. Fu and C. L. Kane, Phys. Rev. Lett. **102**, 216403 (2009).
[50] J. Nilsson, A. R. Akhmerov, and C. W. J. Beenakker, Phys. Rev. Lett. **101**, 120403 (2008).
[51] A. R. Akhmerov, J. Nilsson, and C. W. J. Beenakker, Phys. Rev. Lett. **102**, 216404 (2009).
[52] D. Rainis, L. Trifunovic, J. Klinovaja, and D. Loss, Phys. Rev. B **87**, 024515 (2013).
[53] D. E. Liu, Phys. Rev. Lett. **111**, 207003 (2013).
[54] S. Valentini, R. Fazio, and F. Taddei, Phys. Rev. B **89**, 014509 (2014).
[55] M. Cheng and R. M. Lutchyn, Phys. Rev. B **92**, 134516 (2015).
[56] D. E. Liu, M. Cheng, and R. M. Lutchyn, Phys. Rev. B **91**, 081405 (2015).
[57] E. J. H. Lee, X. Jiang, M. Houzet, R. Aguado, C. M. Lieber, and S. D. Franceschi, Nat. Nanotech. **9**, 79 (2014).
[58] W. Chang, V. E. Manucharyan, T. S. Jespersen, J. Nygård, and C. M. Marcus, Phys. Rev. Lett. **110**, 217005 (2013).
[59] S. R. Plissard, I. van Weperen, D. Car, M. A. Verheijen, G. W. Immink, J. Kammhuber, L. J. Cornelissen, D. B. Szombati, A. Geresdi, S. M. Frolov *et al.*, Nat. Nanotech. **8**, 859 (2013).
[60] L. Levitov and G. Lesovik, JETP Lett. **58**, 230 (1993).
[61] L. S. Levitov, H. Lee, and G. B. Lesovik, J. Math. Phys. **37**, 4845 (1996).
[62] *Quantum Noise in Mesoscopic Physics, Vol. 97 of NATO Science Series II: Mathematics, Physics and Chemistry*, edited by Y. V. Nazarov (Kluwer Academic Publishers, Dordrecht, 1992), pp. 373–497.
[63] W. Belzig and Y. V. Nazarov, Phys. Rev. Lett. **87**, 197006 (2001).
[64] W. Belzig and Y. V. Nazarov, Phys. Rev. Lett. **87**, 067006 (2001).
[65] M. Kindermann and Y. V. Nazarov, Phys. Rev. Lett. **91**, 136802 (2003).
[66] D. A. Bagrets, Phys. Rev. Lett. **93**, 236803 (2004).
[67] A. Komnik and A. O. Gogolin, Phys. Rev. Lett. **94**, 216601 (2005).
[68] A. O. Gogolin and A. Komnik, Phys. Rev. B **73**, 195301 (2006).
[69] A. O. Gogolin and A. Komnik, Phys. Rev. Lett. **97**, 016602 (2006).
[70] Y. Utsumi, D. S. Golubev, and G. Schön, Phys. Rev. Lett. **96**, 086803 (2006).
[71] A. Gogolin, R. Konik, A. Ludwig, and H. Saleur, Ann. Phys. **16**, 678 (2007).
[72] T. L. Schmidt, A. O. Gogolin, and A. Komnik, Phys. Rev. B **75**, 235105 (2007).
[73] I. Klich and L. Levitov, Phys. Rev. Lett. **102**, 100502 (2009).
[74] D. F. Urban, R. Avriller, and A. Levy Yeyati, Phys. Rev. B **82**, 121414 (2010).
[75] R. Sakano, A. Oguri, T. Kato, and S. Tarucha, Phys. Rev. B **83**, 241301 (2011).
[76] L. Weithofer, P. Recher, and T. L. Schmidt, Phys. Rev. B **90**, 205416 (2014).
[77] D. Bagrets and A. Levchenko, Phys. Rev. B **90**, 180505 (2014).

[78] B. Reulet, J. Senzier, and D. E. Prober, Phys. Rev. Lett. **91**, 196601 (2003).
[79] Y. Bomze, G. Gershon, D. Shovkun, L. S. Levitov, and M. Reznikov, Phys. Rev. Lett. **95**, 176601 (2005).
[80] S. Gustavsson, R. Leturcq, B. Simovič, R. Schleser, T. Ihn, P. Studerus, K. Ensslin, D. C. Driscoll, and A. C. Gossard, Phys. Rev. Lett. **96**, 076605 (2006).
[81] T. Fujisawa, T. Hayashi, R. Tomita, and Y. Hirayama, Science **312**, 1634 (2006).
[82] G. Gershon, Y. Bomze, E. V. Sukhorukov, and M. Reznikov, Phys. Rev. Lett. **101**, 016803 (2008).
[83] C. Flindt, C. Fricke, F. Hohls, T. Novotny, K. Netocny, T. Brandes, and R. J. Haug, Proc. Natl. Acad. Sci. USA **106**, 10116 (2009).
[84] N. Ubbelohde, C. Fricke, C. Flindt, F. Hohls, and R. J. Haug, Nat. Commun. **3**, 612 (2011).
[85] V. F. Maisi, D. Kambly, C. Flindt, and J. P. Pekola, Phys. Rev. Lett. **112**, 036801 (2014).
[86] Z.-Z. Li, C.-H. Lam, and J. Q. You, Sci. Rep. **5**, 11416 (2015).
[87] A. Kamenev and A. Levchenko, Adv. Phys. **58**, 197 (2009).
[88] D. Bagrets, Y. Utsumi, D. Golubev, and G. Schön, Fortschr. Phys. **54**, 917 (2006).
[89] A. G. Abanov and D. A. Ivanov, Phys. Rev. B **79**, 205315 (2009).
[90] W. Belzig, Phys. Rev. B **71**, 161301 (2005).
[91] C. Flindt, T. Novotný, A. Braggio, and A.-P. Jauho, Phys. Rev. B **82**, 155407 (2010).
[92] Y. Utsumi, O. Entin-Wohlman, A. Ueda, and A. Aharony, Phys. Rev. B **87**, 115407 (2013).
[93] E. Sela, Y. Oreg, F. von Oppen, and J. Koch, Phys. Rev. Lett. **97**, 086601 (2006).
[94] P. Coleman, Phys. Rev. B **28**, 5255 (1983).
[95] P. A. Lee, N. Nagaosa, and X.-G. Wen, Rev. Mod. Phys. **78**, 17 (2006).
[96] B. Dong, G. H. Ding, and X. L. Lei, Phys. Rev. B **84**, 235408 (2011).